Concentrates from citrus juice obtained by crossflow microfiltration: guidance of the process considering carotenoid bioaccessibility

Sophie di Corcia[1], Claudie Dhuique-Mayer[1,2], Manuel Dornier[1*]

[1] QualiSud, Univ Montpellier, Cirad, Institut Agro, Univ Avignon, Univ La Réunion, Montpellier, France

[2] Cirad, UMR QualiSud, F-34398 Montpellier, France

[*]Corresponding author: manuel.dornier@supagro.fr

ABSTRACT

This work focused on an eco-friendly process to concentrate carotenoids from a citrus juice formulated with clementine and pink grapefruit. It is based on crossflow microfiltration associated with enzymatic liquefaction, diafiltration and pasteurization. The aim was to evaluate the impact of the main operating conditions on the process performance and on the nutritional quality of the final concentrate taking into account the bioaccessibility of β-carotene, β-cryptoxanthin and lycopene. First, the best enzyme/pressure/membrane combination was chosen in order to maximize permeate flux during microfiltration (> 100 $kg.h^{-1}.m^{-2}$ at 2.6 bar with tubular inorganic membranes). Second thanks to a Plackett-Burman experimental design applied to the whole process, we showed the enzymatic dose was the most impacting parameter on carotenoid bioaccessibility and it decreased it. An optimal dose of enzyme had to be defined in order to obtain a good compromise between the process performance and the nutritional quality of the citrus concentrate.

Keywords: clementine/grapefruit based-product, carotenoid bioaccessibility, membrane process performance.

Nomenclature

β_i: bioaccessibility of the carotenoid i (%)

$\partial J_p/\partial MRR$: coefficient of permeate flux instability ($kg.h^{-1}.m^{-2}$)

BC: β-carotene

BCX: β-cryptoxanthin

CMF: crossflow microfiltration

D[4,3]: particle diameter of which the volume corresponds to the average volume of all particles (μm)

D_{10}: diameter below which 10% vol. of the particles are found (μm)

D_{50}: median diameter below which 50% vol. of the particles are found (μm)

D_{90}: diameter below which 90% vol. of the particles are found (μm)

DMR: diamass ratio (mass of distilled water added during the diafiltration stage divided by mass of retentate)

J_p: permeate flux ($kg.h^{-1}.m^{-2}$)

LYC: lycopene

M_{liq}: liquefaction mode (batch or continuous)

MRR: mass reduction ratio

ø_{pore}: average pore diameter of the membrane (μm)

P_0: pasteurization value (min)

RAE: retinol activity equivalent (μg/250g)

RAE*: retinol activity equivalent taking into account carotenoid bioaccessibility (μg/250g)

RDA: recommended dietary allowances (%)

SIS: suspended insoluble solids ($g.kg^{-1}$)

Span: indicator of the width of the size distribution of the particle diameters (Equation 1)

TA: titratable acidity ($g.kg^{-1}$)

T_{CMF}: temperature of crossflow microfiltration (°C)

51 TDM: total dry matter ($g.kg^{-1}$)

52 t_{liq}: enzymatic liquefaction time (min)

53 T_{liq}: temperature of enzyme liquefaction (°C)

54 TmP: transmembrane pressure (bar)

55 TSS: total soluble solids ($g.kg^{-1}$)

56 U: crossflow velocity ($m.s^{-1}$)

1. Introduction

Citrus are the most cultivated fruits in the world and many varieties are produced (orange, grapefruit, mandarins, tangerines, lemons and limes). A large amount of citrus fruits is consumed worldwide in juice form. The consumption of citrus juices has grown rapidly since the '80s, from a consumption of 3 to 22 L per year and inhabitant in Europe today (AIJN - Market Report 2017). Moreover, 75% of citrus fruit production in Brazil, the top producing country in the world, is processed into juice (USDA - World Markets and Trade 2020). Consumers perceive citrus juices, especially orange juice, as a natural source of vitamin C and minerals, but they are also rich in a large variety of phytochemicals such as carotenoids. Carotenoids are liposoluble pigments synthesized mainly by plants and stored in the chromoplasts of plant cells in a solid-crystalline state or in a liquid-crystalline form and/or a lipid-dissolved form (R. M. Schweiggert, Mezger, Schimpf, Steingass, & Carle, 2012). Chromoplast morphology also varies (globular, crystalline, membranous, fibrillary and tubular) depending on the fruit, and between different tissues of the same fruit (R. Schweiggert & Carle, 2017; Zhang et al., 2019). In addition to giving an attractive color to citrus juice, carotenoids have many health benefits: antioxidant, antidiabetic, anti-inflammatory and anti-cancer (Bungau et al., 2019; Lee, Hu, Park, & Lee, 2019; Sun, Tao, Huang, Ye, & Sun, 2019). Several studies have also shown that the consumption of carotenoid-rich food is linked to a reduced risk of developing certain chronic diseases such as cardiovascular disease, cataracts or cancer (Lee et al., 2019; Rodriguez-Concepcion et al., 2018; Carla M Stinco et al., 2019). However, the most relevant role is the pro-vitamin A activity attributed to carotenoids containing at least one unsubstituted β-ionone ring such as α-carotene, β-carotene and β-cryptoxanthin and can be converted into vitamin A by the specific enzyme β-carotene oxygenase. Vitamin A plays a key function in vision, embryonic development, reproduction and cellular growth and differentiation (Kopec & Failla 2018). Although carotenoids are present in significant amounts in citrus juices, their health effects are limited by their bioavailability including their bioaccessibility. Carotenoid bioaccessibility, which is one of the main factors governing bioavailability, corresponds to the proportion of carotenoids released from the food

matrix and transferred into mixed micelles that can be then absorbed by the human intestinal cells (Poulaert, Borel, Caporiccio, Gunata, & Dhuique-Mayer, 2012). Therefore, carotenoids must be released from the chromoplasts in order to reach the lipid phase and be incorporated into the mixed micelles and be available for intestinal absorption. In fact, bioavailability depends on several factors among which food matrix and its technological processing are the more important. Some studies have shown that the release of carotenoids from their food matrix was strongly influenced by the physical shape of the chromoplasts (R. Schweiggert & Carle, 2017; R. M. Schweiggert et al., 2012; Zhang et al., 2019). Better liberation and bioaccessibility of carotenoids from non-crystalline chromoplasts was reported by Schweiggert, Mezger et al. 2012. On the other hand, mechanical and thermal treatments applied to foods can modify their nutritional quality and increase carotenoid bioaccessibility (Barba, Saraiva, Cravotto, & Lorenzo, 2019; Cilla et al., 2012; Knockaert, Lemmens, Van Buggenhout, Hendrickx, & Van Loey, 2012; Kopec & Failla, 2018). These treatments destroyed cell structure, from the cell wall to the membrane of organelles such as chromoplast membranes promoting carotenoid release. Thermal treatments, widely used in food industry for stabilization and preservation, conduce to cell disorganization mainly through depolymerization and solubilization of pectic polysaccharides (Lemmens, Van Buggenhout, Oey, Van Loey, & Hendrickx, 2009) that has led to better understand the effects on carotenoid bioaccessibility. Other studies showed that cooking and grinding can increase lycopene bioaccessibility (J. Aschoff et al., 2015; J. K. Aschoff et al., 2015; Carla M. Stinco et al., 2012; Carla M Stinco et al., 2019). The impact of the process has also been studied on citrus juices: the carotenoid bioaccessibility in pasteurized juices is higher than in fresh juices (J. K. Aschoff et al., 2015; Carla M. Stinco et al., 2012). Moreover, for humans, the bioavailability of β-carotene and β-cryptoxanthin is higher for pasteurized orange juice than for fresh juice (J. Aschoff et al., 2015).

Crossflow microfiltration (CMF), an eco-friendly membrane process, allows the clarification and stabilization of fruit juices (Dornier, Belleville, & Vaillant, 2018; Maktouf et al., 2014; Mierczynska-Vasilev & Smith, 2015) as well as the concentration of hydrophobic compounds without heating

(Chaparro et al., 2016; de Abreu et al., 2013; Polidori, Dhuique-Mayer, & Dornier, 2018). Indeed, hydrophobic compounds, which are associated with insoluble solids, are generally retained by the membrane. Thus, it is possible to increase carotenoid content in retentate up to 10 fold by using this physical separation process to obtain a carotenoid-rich concentrate without heating or using organic solvent.

However, this process results in a concentrate with physical characteristics that are considerably different from those of juice and so could affect carotenoid bioaccessibility. In addition, viscosity and pectin content increase with increasing carotenoid content during CMF. L. Gence, Servent, Poucheret, Hiol, and Dhuique-Mayer (2018) have already compared the effect of CMF on the carotenoid bioaccessibility between concentrates made with fresh and pasteurized juices and they showed that bioaccessibility was strongly correlated to the pectin content and structure. The aim of this study was to go further and to focus on a more complete process including the CMF step and several other unit operations (enzymatic liquefaction, diafiltration and pasteurization). Within this context, the work expected to evaluate the impact of the main operating conditions on process performance and on nutritional quality of the final concentrate through carotenoid bioaccessibility in order to optimize the process. This one, including various steps, was originally guided by carotenoid bioaccessibility for the production of citrus concentrates. Another main goal was to understand how different processing steps could affect carotenoid bioaccessibility.

2. Materials and methods

2.1. Materials

Flash-pasteurized clementine *(Citrus clementina* Hort. ex Tan.) and pink grapefruit (*Citrus paradisi* Macf.) juices were purchased in a local supermarket (Saint-Clément de Rivière, France). Packaged in aseptic carton packs, these industrial 100% pure juices, i.e. without any additives in accordance with current regulations, were stored at 4 °C for two weeks before processing (no significant change in carotenoid profile highlighted during storage). A formulation obtained from 60/40 (v/v) *C. clementina* / *C. paradisi* juices was chosen in order to obtain a product containing at a time the 3 carotenoids β-cryptoxanthin, β-carotene and lycopene each with an interesting concentration on a nutritional point of view. Three different lots of juice were purchased with volumes ranging from 10 kg to 50 kg.

2.2. Processing

All the unit operations constituting the process are detailed in **Figure 1**. Citrus juices underwent several operations, the main one being crossflow microfiltration (CMF). First, an enzymatic pre-liquefaction of the juices was carried out in order to decrease viscosity and limit membrane fouling during CMF. Widely used in the juice industry, this step guarantees good performance of the process (F. Vaillant et al., 1999). After concentration of carotenoids by microfiltration, a diafiltration step allowed the purification of the carotenoids by removing soluble solids, mainly sugars and organic acids. A final pasteurization step was added to stabilize the product eliminating the microorganisms retained in the concentrate.

2.2.1. Enzymatic liquefaction

153 Two commercial enzyme mixtures, Ultrazym AFP and Pectinex Ultra SP from Novozymes (Denmark),
154 commonly used for filtration and clarification of fruit juices (Sandri, Fontana et al. 2011, Bajpai 2012),
155 were compared. They consist of a mixture of enzymes (mainly pectinases associated with secondary
156 activities such as hemicellulases) that allow the hydrolysis of the structural polysaccharides of cell
157 walls especially pectic compounds. Activity spectra of these two mixtures are different with
158 pectinesterase as preponderant activity for Pectinex and polygalacturonase for Ultrazym (Macedo,
159 Robrigues, Pinto, & de Brito, 2015). Citrus concentrates were treated with enzymes (50 - 300 µL kg^{-1})
160 either prior to microfiltration (batch) or during microfiltration (continuous) ($\mathbf{M_{liq}}$), at a temperature
161 $\mathbf{T_{liq}}$ of 30 or 50°C. In the batch mode, all the juice was treated with enzyme prior to microfiltration for
162 45-90 min while in the continuous mode the system was continuously fed by juice and enzyme (for
163 every 100 g of permeate discharged, feeding by 100 g of juice with enzyme).

164

165 **2.2.2. Concentration by crossflow microfiltration and purification by diafiltration**

166 The crossflow microfiltration device (TIA, Bollène, France), described by Polidori et al. (2018), was
167 constituted of a 3 L feed tank, connected to 4 housings each containing a single-tubular ceramic
168 membrane mounted in series (**Table 1**). The crossflow circulation of the suspension was ensured by a
169 positive displacement pump with an eccentric rotor (model PCM, Moineau, Levallois-Perret, France).
170 The temperature of the juice in the pilot unit (T_{CMF}) was regulated by a jacketed heat exchanger
171 connected to a cryostat (model F34, Julabo GmbH, Seelbach, Germany). The transmembrane
172 pressure (TmP), controlled by a backpressure valve, was measured using manometers located at the
173 inlet and the outlet of the circulation loop. The crossflow velocity (U) in the loop could vary from 2 to
174 5 $m.s^{-1}$ thanks to a frequency converter connected to the pump. Depending on the purpose of the
175 filtration test, the trial could be conducted at a constant mass reduction ratio MRR of 1 (total
176 recycling of permeate and retentate, i.e, without concentration) or increasing MRR (removing
177 permeate and compensating with raw juice in the feed, i.e., with concentration). In that case, the

permeate flux J_p was monitored as a function of MRR. In order to facilitate comparisons between the trials, the average permeate flux between MRR 3 and 4.4 was chosen. A permeate flux instability coefficient $\partial J_p/\partial MRR$ was defined as the slope of J_p as a function of MRR. The lower the coefficient, the more stable the permeate flux.

A diafiltration step can follow concentration in order to purify retentate using distilled water as a solvent. After concentration up to MMR 4.4, diafiltration was conducted with a constant volume compensating the mass of extracted permeate by an equal mass of distilled water added to the feed tank. The diamass ratio (DMR) was defined as the ratio between the total mass of distilled water added to the tank and the mass of circulating retentate. In our trials, diafiltration was stopped when the DMR reached approximately 1.0.

2.2.3. Pasteurization

According to Gates (2012) and the standard practices in the industry, citrus concentrates were pasteurized choosing a pasteurization value $\mathbf{P_0}$ of 100 min as a target (reference temperature 70°C and z-value 10°C). The concentrate was distributed in several 15 mL glass tubes and put in a water bath at 80°C. Thanks to a thermal probe placed into one tube, the temperature of the concentrate was measured every minute and the P_0 was calculated according to the standard Ball procedure. When the targeted P_0 was reached (after 14 min), the tubes were quickly immersed in an ice-cold water bath to cool down and stop the treatment.

199 **2.3. Analyses**

200

201 **2.3.1. Physico-chemical parameters**

202 *pH and titratable acidity*

203 The pH of citrus juices and concentrates and their titratable acidity were measured using a Titroline
204 titrator (Schott Schweiz AG, St. Gallen, Switzerland). The pH was measured with a pH probe,
205 previously calibrated with buffer solutions of pH 4 and 7. The titratable acidity was measured by
206 titration with 0.1 mol.L^{-1} NaOH up to pH 8.3 and expressed as citric acid content per kg of juice or
207 concentrate.

208

209 *Soluble and insoluble fractions*

210 Juices and concentrates were analyzed for total soluble solids (TSS) using a refractometer at 25°C
211 (Pocket PAL-1, 0-53% Brix, ATAGO, Tokyo), total dry matter (TDM) (2.0 g of concentrate dried in an
212 oven at 70°C under vacuum at 100 mPa for 24 h) and suspended insoluble solids (SIS). For SIS, 5.0 g
213 of concentrate were weighed in previously weighed 15 mL falcon tubes. The samples were then
214 centrifuged at 1900 x g, for 20 min, at room temperature (centrifuge 5810 R, Eppendorf, Hamburg,
215 Germany). After centrifugation, the supernatant was removed in order to retain only the insoluble
216 particles in the pellet. Then, the pellet was washed twice in succession with water: it was re-
217 suspended in 10 mL of distilled water, vortexed and centrifuged for 20 min. The supernatant was
218 removed and the last pellet was dried in an oven at 70°C for about 24 h. The mass ratio between the
219 dry base and the initial quantity thus represents the SIS content.

220

221 *Rheological properties*

Flow rheological measurements were carried out on juices and concentrates with a Physica imposed stress rheometer (model MCR301, Anton Paar Gmbh, Graz, Austria), equipped with a duvet geometry measurement module (double concentric cylinder, ref. DG27 / T2000 / SS) and accompanied by Rheoplus software for data acquisition. The temperature was regulated at 25°C using a Peltier effect system connected to a refrigerant (Viscotherm VT2, Anton Paar Gmbh, Graz, Austria). The limit apparent viscosity for a shear rate of 1000 s^{-1} was chosen to compare concentrates. Indeed, this value is close to that evaluated on the membrane surface in the CMF system (Dahdouh et al., 2015).

Particle size and distribution

Measurements of juice particle size were made with a Laser diffraction granulometer (Mastersizer 3000, Malvern Instruments Limited, Worcestershire, UK). Values of 1.73 and 1.33 were used respectively as refractive indices for particles and the liquid phase of the suspension, the particle absorption index being 0.1. (Corredig, Kerr, & Wicker, 2001; Dahdouh, Delalonde, Ricci, Ruiz, & Wisnewski, 2018). The samples were diluted, introduced into the feed tank with an obscuration value of about 30% for juices and 15% for concentrates and then agitated at 1500 rpm. In these experimental conditions, the particle size distribution was assumed not to be affected. For each measurement, the particle size distribution was obtained in volume. The mean volume diameter D[4,3], which indicates the particle diameter of which the volume corresponds to the average volume of all the particles in the sample (called the DeBrouckere mean), was deducted from the measured distribution. The span, that characterizes the width of the distribution of particle sizes in the suspension was also calculated (Equation 1).

Equation 1

$$Span = \frac{D_{90} - D_{10}}{D_{50}}$$

with D_{50} the median diameter, D_{10} and D_{90} the diameters below which 10% and 90% of the particles are found.

Turbidity

The turbidity was measured using a turbidimeter (model LP 2000, Hanna instruments, Szeged, Hungary) which measures the intensity of the light (890 nm) scattered by the suspension, the angle between the detector and the light source being 90°. Before each measurement, the turbidimeter was calibrated using two standard formazin solutions at 0 and 10 NTU. Measurements were made on concentrates diluted 30 folds in distilled water in order to respect the accuracy range of the turbidimeter and results were expressed taking into account the dilution factor.

2.3.2. Carotenoid analysis

2.3.2.1. Carotenoid content

Extraction

Carotenoid extraction, carried out according to the method described by Gies, Descalzo, Servent, and Dhuique-Mayer (2019), has been optimized and applied to citrus juices and concentrates. Two g of juice or 0.5 g of concentrate mixed with 0.5 mL distilled water were homogenized in a glass tube (20 mL). Two mL ethanol with 1% pyrogallol were added and then the mixture was vortexed (homogenized). The tube was then placed in a water-bath at 70°C for 2-3 min, protected from light. Two mL of KOH 12 $mol.L^{-1}$ was added and the mixture was vortexed and set in a water bath at 70°C for 30 min. After cooling in an ice bath, 2 mL of distilled water was added to help the phase shift. The extraction was carried out twice with 5 mL of hexane. The hexane phase was pooled and evaporated under nitrogen in a water bath at 37°C. The dry extracts were dissolved in 500 µL of CH_2Cl_2 and 500

µL of methyl tert-butyl ether (MTBE)/methanol mixture (4:1, v/v) in an amber vial before injection in HPLC.

HPLC analysis

HPLC carotenoid analyses were performed according to a previous study (Poulaert et al. 2012) with an Agilent 1100 system equipped with a diode array detector and autosampler. The column used was a C30 YMC column (250 x 4.6 mm; 5 µm, YMC Europe GMBH, Germany). The flow rate was 1 $mL.min^{-1}$, the analysis temperature 25°C and the injection volume 20 µL. The mobile phases were water (eluent A), methanol (eluent B) and MTBE (eluent C) that follow the gradient described by Gleize, Steib, André, and Reboul (2012). The absorbance was measured at 450 nm to identify β-carotene (BC), β-cryptoxanthin (BCX) and 470 nm for lycopene (LYC). Chromatographic data and UV-Visible spectra (Agilent ChemStation Plus software) allowed the different carotenoids to be identified. Quantification of carotenoids was achieved using external calibration curves with 5 concentration levels from 2 to 15 $mg.L^{-1}$ for the BC standard, from 10 to 40 $mg.L^{-1}$ for BCX and from 7 to 50 $mg.L^{-1}$ for LYC.

2.3.2.2. Carotenoid bioaccessibility

In vitro digestion

The *in vitro* digestion model used in our study was initially developed by Reboul et al. (2006) especially for carotenoids. It had been validated against human studies and was considered to be a reliable model for carotenoid behavior during *in vitro* digestion (Etcheverry, Grusak, & Fleige, 2012). This model was adapted for citrus juices according to Dhuique-Mayer et al. (2007). Briefly, 30.0 g of juice or 5.0 g of concentrate were mixed with 32 mL of a 0.9% NaCl solution. The mixture was incubated in a stirring water bath at 37°C for 10 min, and protected from light. To simulate the gastric digestion phase, the pH was adjusted to 4.0 with 1 $mol.L^{-1}$ NaOH, then 2 mL of pepsin was added before incubating the mixture at 37°C for 30 min. To simulate the duodenal phase, the pH of

295 the gastric mixture was raised to 6.0 by adding 20 mL of 0.45 mol.L^{-1} sodium bicarbonate. Then, 9 mL
296 of a solution containing porcine pancreatin (2 mg.mL^{-1}) and porcine bile extract (12 mg.mL^{-1}) in 100
297 mmol.L^{-1} trisodium citrate were added, as well as 4 mL for juice or 2 mL for concentrate of porcine
298 bile extract (0.1 g.mL^{-1}) and 1 mL of cholesterol esterase (10 mg at 32 Unit.mL^{-1} in 6 mL of distilled
299 water). Samples were subsequently incubated in a shaking water bath at 37°C for 30 min to finish the
300 digestion process. Micelles were separated by centrifugation at 48 000 x g for 4 h at 10°C using an
301 Avanti JE rotor JA-20 (Beckman-coulter, USA), and the aqueous fraction was collected and filtered
302 through a 0.20 µm filter (Whatman, U.K.). Aliquots were stored at -20 °C until analysis.

303

304 *Carotenoids from Micellar phase analysis*

305 Carotenoid extraction from digested samples was performed as previously described by Dhuique-
306 Mayer et al. (2018). An aliquot of 10 mL of the micellar phase from a digested sample was extracted
307 3 times with 10 mL of hexane and 5 mL of ethanol containing 100 µL of β-apo-8'-carotenal (at 24.4
308 mg.L^{-1}) as an internal standard. The collected hexanic phases were dried with anhydrous sodium
309 sulphate. The pooled hexane extracts were evaporated and dissolved in 250 µL of CH_2Cl_2/250 µL of
310 the MTBE/methanol (4:1, v/v) before HPLC analysis according to the analytic conditions described
311 below for carotenoid analysis.

312 Bioaccessibility of a carotenoid i, noted β_i, was calculated according to Equation 2 and expressed in
313 percentage (%).

314 *Equation 2*

315 $$\beta_i = 100 \frac{m_i}{m_{i0}}$$

316 m_i: amount of carotenoid i in the micellar phase (mg)

317 m_{i0}: amount of carotenoid i in the initial sample of citrus juice or concentrate (mg)

318

2.3.3. Vitamin A activity equivalent calculation

Vitamin A activity equivalent was expressed in terms of retinol activity equivalents RAE (Equation 3). The RAE value was widely used for food. Another vitamin A activity equivalent RAE*, taking into account carotenoid bioaccessibility, was defined using Equation 4. Results were referred to 250 g of product corresponding to an average glass of beverage. Moreover, the percentage of Recommended Dietary Allowances (RDA) provided by 250 g of juice or concentrate could be deduced considering that 800 µg of RAE is recommended for an adult (> 18 years old) per day (Medicine, 2001) (National Institutes of Health, Office of Dietary Supplements, 2020).

Equation 3

$$RAE = \frac{[\mathrm{BC}] \times 250}{12} + \frac{[\mathrm{BCX}] \times 250}{24}$$

Equation 4

$$RAE^{*} = \frac{[\mathrm{BC}] \times 250}{12} \times \frac{\beta_{BC}}{100} + \frac{[\mathrm{BCX}] \times 250}{24} \times \frac{\beta_{BCX}}{100}$$

[BC]: β-carotene content ($mg.kg^{-1}$)

[BCX]: β-cryptoxanthine content ($mg.kg^{-1}$)

β_i: Bioaccessibility of carotenoid i (%)

2.4. Experimental approach

The chosen experimental strategy was organized in 3 successive phases:

- the first phase focused on the CMF operation. It aimed to choose the 3 main operating parameters, i.e., membrane, transmembrane pressure (TmP) and enzyme mixture. It was based mainly on the permeate flux without considering carotenoid bioaccessibility in order to reduce the screening and restrict the field of the study. So, it was assumed that the membrane and transmembrane pressure do not alter the characteristics of the suspension and therefore the carotenoid bioaccessibility. This

assumption considered the retentions of the main compounds of juices are close to each other for the 4 tested membranes, i.e. retentions are only little affected by fouling, even if it can be a little different from one membrane to another (Dornier et al., 2018; Hofs, Ogier, Vries, Beerendonk, & Cornelissen, 2011). The enzyme mixture effect was restricted in this part because it was not possible to modulate the activity profile and this was not the core of the work. The used process combined an enzymatic treatment in batch mode with the comparison of both pectinolytic mixtures (300 µL.kg^{-1}, 45 min, 30°C) and crossflow microfiltration at MRR 1 (1.8 - 3.5 bar, 1 m.s^{-1}, 30°C). Thus, for the four membranes, with different TmP and enzymatic treatment, the performance of the operation was assessed measuring permeate flux, J_p, as well as the physico-chemical characteristics of juice in order to select the best membrane/TmP/enzyme combination.

- the second phase considered the complete process. It aimed to identify the other operating parameters that most influence carotenoid bioaccessibility, permeate flux and physico-chemical properties of citrus concentrates thanks to a fractional factorial experimental design of Plackett-Burman (Goupy, 2006; Vanaja & Shobha Rani, 2007). The process combined i) an enzymatic liquefaction with the preselected enzyme mixture at 300 µL kg^{-1} ii) a crossflow microfiltration operation using the preselected membrane/TmP combination with or without diafiltration, iii) a possible additional step of pasteurization. Seven operating parameters were modulated: enzymatic liquefaction conditions (dose of enzyme, temperature, implementation mode), CMF conditions (crossflow velocity, temperature), and with or without diafiltration and pasteurization alone or in combination (**Table 2**). Statistical analyses were performed from means and standard deviations using XLSTAT software 2016. Statistical significance was tested using one-way analysis of variance with a post-hoc Fisher's test. A P value < 0.05 was considered statically significant. From a Plackett-Burman experimental design, the effects of each factor were calculated by multiple linear regression using MS-Excel between the lowest and the highest level [-1, 1]. Relative effects were obtained dividing them by the mean value (expressed in %).

- The last phase aimed to investigate further the process focusing on the most influent operating conditions and considering simultaneously carotenoid bioaccessibility and process performance.

3. Results and discussion

3.0. Initial citrus juice characterization

As a reminder, an initial standardized citrus juice was formulated by mixing clementine and grapefruit juices with a ratio of 60/40% in order to nutritionally optimize the carotenoid profile. So, raw citrus juice was characterized to later assess the effect of processing on the concentrates. Physico-chemical analysis, carotenoid content and bioaccessibility of citrus juices were assessed (**Table 3**). Juice from lot A was used for the first phase, lot B was used for the second and third phase and the last juice from lot C was only used for the third phase. Note that with regard to the physico-chemical and structural parameters, juices from the different lots were very similar whereas their carotenoid content and bioaccessibility differed significantly. The impact of lot appeared greater for carotenoid content and bioaccessibility which were more affected by a possible difference in fruit maturity before processing or by several slight variations in processing between lots.

Physico-chemical and structural parameters

The pH of citrus juices was acid which facilitates their preservation. A fruit juice is a suspension, i.e. a solid-liquid dispersion. It is a heterogeneous and unstable mixture due to the existence of two phases: the dispersing phase, water with TSS (soluble fraction) and the dispersed phase with SIS (colloidal, supra-colloidal and particulate fractions). The dispersing phase occupies almost all the juice and is mainly composed of carbohydrates and organic acids (Dahdouh, Delalonde, Ricci, Rouquie, & Wisniewski, 2016). Note that TSS was close to that of grapefruit or orange juice (95 and

100 g.kg^{-1} respectively). The average ratio TSS/SIS, which is an essential characteristic for carotenoid purification by CMF, was about 33 (Servent, Abreu, Dhuique-Mayer, Belleville, Dornier, 2020). The SIS corresponded to the pulp in juices and represented the particulate fraction with particle size over 100 µm. By the way, the mean volume diameter of citrus juice was high (about 900 µm). Regarding the viscosity, juices behaved as rheofluidifiers with a low viscosity equal to 2-3 mPa.s, which is very close to that of pure water.

Carotenoid analysis

Carotenoid content and bioaccessibility were very different for the three carotenoids. Citrus juices contained three main carotenoids where lycopene provided by grapefruit had the highest concentration (in average for lots B and C, 5.55 mg.kg^{-1}) followed by the two provitamin A carotenoids: β-cryptoxanthin (2.85 mg.kg^{-1}) and β-carotene (1.29 mg.kg^{-1}) mainly provided by clementine (**Table *3***). The addition of grapefruit juice to clementine juice resulted in a balanced carotenoid composition by increasing β-carotene and providing lycopene (Poulaert et al., 2012). On the other hand, carotenoid bioaccessibility varied between the three carotenoids in the following order: BCX > BC > LYC. Carotenoid bioaccessibility strongly depends on carotenoid type (carotene or xanthophyll) and this order is in agreement with literature, whatever the food source. Indeed, xanthophylls (BCX), which are less hydrophobic than carotenes, are located at the surface of lipid droplets which means they are released more easily from lipid droplets and therefore, more easily incorporated into mixed micelles (Tyssandier, Lyan, & Borel, 2001). Furthermore, although lycopene content was the highest, its bioaccessibility was the lowest (< 1%). The low bioaccessibility of lycopene could be due to the morphology of chromoplasts. Indeed, a recent study has shown that chromoplasts with crystalline morphology accumulated in red-fleshed grapefruits with an extremely high accumulation of lycopene (96%) (Zhang et al., 2019). Furthermore, fruits with high carotenoid content in crystalline chromoplasts had lower bioaccessibility than the others which accumulated

high content of carotenoid in globular chromoplasts (R. M. Schweiggert et al., 2012). Regarding the RAE, the consumption of 250 g of juice provided an average of 55 µg of vitamin A equivalent which corresponds to about 8% of the Recommended Dietary Allowances (RDA). These values were very similar to those obtained with homemade orange juice where RAE was about 43 µg for a glass of 250 g, i.e. 5.4% of RDA (Carla M. Stinco et al., 2012) but were considerably less than carrot juice which provides 1690 µg per 250g (211.3% of RDA). Taking into account the bioaccessibility, the RAE* of citrus juice was drastically divided by approximately 5 which corresponds to only 1.8% of the RDA. Finally, RAE overestimates the contribution of vitamin A. It is relevant to take into account carotenoid bioaccessibility to more accurately assess the provitamin A equivalent provided by food.

3.1. Selection of enzyme, transmembrane pressure and membrane combination

3.1.1. Influence of enzymatic treatment on permeate flux and structural characteristics of juices

Permeate flux

Stabilized permeate flux obtained during crossflow microfiltration of the untreated citrus juice and the juice previously treated with both commercial enzymes, Ultrazym and Pectinex, are presented in **Table 4**. In all the tested cases, enzymatic liquefaction enhanced the permeate flux. Considering that repeatability of permeate flux measurements using this type of well-controlled pilot equipment is between 5 and 10%, enzyme treatment allowed to increase J_p for the membranes PALL, ORELIS and TAMI significantly (J_p multiplied by 1.17 to 1.54). Except for the ORELIS membrane, the results indicated there was no significant difference in permeate flux between both enzymes. Many studies showed that pectinolytic enzymes such as Ultrazym or Pectinex, thanks to soluble pectin depolymerization and damage to the cell wall polysaccharides, have long been used to decrease viscosity, to limit the fouling power of fruit juices and therefore, to increase filtration performance

(Ushikubo, Watanabe, & Viotto, 2007; F. Vaillant et al., 1999; Yu & Lencki, 2004). In addition, Chaparro, Dhuique-Mayer et al. (2016) explained the permeate flux rise by disorganizing the gel-like structure that can be formed at the surface of the membrane, facilitating mass transfers through the porous media. The ST-GOBAIN membrane clearly differed from the others because the flux was not significantly modified after enzyme treatment with this membrane. This variation in behaviour can be linked to a different fouling mechanism of this membrane because, on the one hand, of its larger average pore diameter more favourable to internal fouling (0.6 µm instead of 0.2 µm) and, on the other hand, of the very different nature of the membrane material (silicon carbide instead of metal oxides) which probably did not lead to the same interactions with the product.

Physico-chemical and structural parameters

Neither enzymatic liquefaction (whatever mixture is used) nor crossflow microfiltration (30°C, 2.6 bar, MRR 1, 5 $m.s^{-1}$) modified pH, TSS, AT, TDM, SIS or turbidity (**Table S1**).

Particle size spectra comparison (**Figure S1**) showed enzymatic liquefaction drastically decreased the particle volume diameter of citrus juices: D[4,3] was reduced from 6 up to 9 fold (**Figure 2**). Indeed, the particulate fraction (> 100 µm) was degraded and replaced by the supra-colloidal fraction (< 100 µm). Enzymatic liquefaction with Ultrazym had a stronger effect than with Pectinex on particle size distribution: particle size was 4 fold lower with Ultrazym than with Pectinex. Without using enzymes, it could be observed that the high shear rates during crossflow microfiltration considerably decreased particle size of untreated citrus juice as also shown by Dahdouh et al. (2016) but not as much as enzymatic liquefaction. It was also noted that particle size in the juices that have undergone microfiltration in addition to an enzymatic treatment was similar to those that have undergone only the enzymatic treatment.

Regarding particle size dispersion, the span was low for the raw juice mainly characterized by a single peak of large particles (> 1000 µm), and increased slightly for microfiltered juice that gave bimodal

distribution (two main populations at around 100 and 900 µm). For juices treated with enzymes, either microfiltered or not, the span was higher than untreated juices, characterized by no peak and particle sizes ranging from 5 to 900 µm.

Enzymatic liquefaction decreased viscosity by 30% but no significant difference between the two enzymes, Ultrazym and Pectinex, was observed (**Figure 3**). Similar results were found by Vaillant, Millan, O'Brien et al. in passion fruit juice (F. Vaillant et al., 1999). This phenomenon is well known (Kuddus, 2018) and is related to the actions of pectinolytic enzymes on the soluble pectin fraction and also on the pectic compounds entrapped in the cell walls that make up the bulk of suspended insoluble solids. Through hydrolytic cleavage (polygalacturonase activity), non-hydrolytic breakdown (pectin-lyase activity) or deesterification (pectinesterase activity), these enzymes contribute to decrease molar mass of pectins and chemical interactions between biopolymers chains (mainly H-bonds) what leads to a viscosity drop (Jayani, Saxena, & Gupta, 2005) .

On the other hand, crossflow microfiltration did not modify either the viscosity of the untreated juice or the viscosity of the juices previously treated with enzymes. Due to the constant MRR (equal to 1), the rheological properties of juice were not much affected by microfiltration. Note that only particle size was modified by microfiltration, suggesting that there was no correlation between particle size distribution and viscosity. Moreover, for a constant MRR, the effect of enzymatic treatment on viscosity was greater than that of microfiltration.

Thanks to the degradation of the cell wall polysaccharides, together with that of the soluble pectins, enzymatic treatments considerably modified the physical characteristics of the suspension. Particle size and viscosity of juice were decreased that was, in our case, favorable for mass transfers through the membrane and was conducive to higher permeate fluxes (Ushikubo et al., 2007; F. Vaillant et al., 1999; Yu & Lencki, 2004). Thus, using pectinolytic enzymes is an interesting way to improve process performance.

3.1.2. Effect of TMP on permeate flux and structural characteristics of juices pre-liquefied with enzymes

Permeate flux

The comparison of permeate flux for different transmembrane pressures and membranes was made in a pressure range between 0.8 and 4.3 bar (**Figure 4**). As provided by Darcy's law, at constant MRR, permeate flux increased by increasing the transmembrane pressure that corresponds to the driven force for mass transfers through the porous medium. Nevertheless, permeate flux was not proportional to TmP and, a plateau was reached when TmP increased. So an optimal pressure over which it is not interesting to filtrate the product could be defined (around 3 bar in our case). These results, that could be explained by the increasing hydraulic resistance of the fouled membrane with pressure, are very usual and are in accordance with many studies such as Cisse et al. 2011 (Cisse, Vaillant, Soro, Reynes, & Dornier, 2011) who also have specified that the transmembrane pressure effect varied according to the MRR. The TAMI membrane gave the highest permeate flux under any TmP, followed by ST-GOBAIN and PALL which had similar permeate flux trends and then the ORELIS membrane. These differences between the membrane behavior were surely due to their different structural characteristics (thickness, porosity, tortuosity, pore diameter distribution, surface state) and to the different materials that could be more or less favorable to physico-chemical interactions with juice components. Surprisingly, the ST GOBAIN membrane was not the most effective even if it showed a much higher water permeability than the others and a larger average pore diameter. As often shown in many cases in microfiltration (Cheryan, 1998), this difference could be related to its higher average pore diameter that promotes the internal part of membrane fouling (through pore constriction and/or blocking) and so create a higher hydraulic resistance of the system.

From TmP of 3 bar, permeate flux were higher than 100 $kg.h^{-1}.m^{-2}$, for all the membranes, that was an encouraging value for industrial application of the process. TAMI membrane showed promise

516 from an energy point of view because it was able to filtrate at a lower transmembrane pressure while
517 guaranteeing a higher permeate flux.

518

519 *Physico-chemical and structural parameters*

520 As might be expected, transmembrane pressure did not cause any modifications of juice
521 characteristics. Shear stress variations induced by passing through the pressure regulating valve was
522 probably negligible compared to the shear stress generated by high fluid velocity into the circulation
523 loop.

524

525 Finally, TAMI membrane was selected guaranteeing the best permeate flux at low transmembrane
526 pressure. By the way, an average transmembrane pressure of around 2.5 bar was chosen to ensure
527 high filtration performance while maintaining an acceptable energetic cost for the process.

528 Due to the similar effects of the two enzymes on performance filtration, the choice of enzymatic
529 treatment was oriented towards Ultrazym. It further reduced the particle size of juice and low
530 particle size appeared to induce better permeate flux.

531 Having found this enzyme/membrane/transmembrane pressure combination, it is possible to go
532 further with the process and optimize it in order to obtain concentrates with the best carotenoid
533 bioaccessibility and therefore with the highest nutritional qualities.

534

535 **3.2. Selection of the most influential factors on carotenoid bioaccessibility**

536

537 **3.2.1. Process performance and concentrate characteristics**

In this part of the study, crossflow microfiltration was carried out concentrating the product in the retentate loop up to a MRR of 4.4.

Permeate flux

Results showed permeate flux varied from 15 to 120 $kg.h^{-1}.m^{-2}$. It was logically the lowest for the C8 concentrate that was the least treated concentrate (no enzymatic liquefaction, no diafiltration, low crossflow velocity and filtration temperature) contrary to the C4 concentrate (**Table 5**). Regarding the stability of permeate flux, the C8 concentrate appeared to be the one with the most stable permeate flux, followed by C1 and C2. The higher stability of permeate flux observed with the concentrate C8, could be related to the softer operating conditions used (low temperature and crossflow velocity, no enzyme treatment) and to the low permeate flux that could favor a more progressive fouling of the membrane during the concentration. On the contrary, C3, C5, C6 were characterized by a high coefficient of instability $\partial Jp/\partial MRR$. No correlation between permeate flux and stability was observed. Of course, the higher and more stable the permeate flux the better the process for industrial application (cf. some examples **Figure S2**).

Physico-chemical and structural parameters

Several parameters were evaluated in juice and in the 8 concentrates at MRR 4.3 (Table 5). Firstly, insoluble solids were completely retained by the membrane and increased about 4-fold in concentrates compared to the juice, that is logically close to the MRR attained. Turbidity values were also multiplied by 4 in concentrates, which was in line with a study by Vaillant et al. 2008, which showed that in certain cases, turbidity appears to be a good SIS substitute (Fabrice Vaillant, Pérez, Acosta, & Dornier, 2008). To purify the micronutrients, a step of diafiltration was added following crossflow microfiltration for four concentrates (C2, C4, C5, C6). As expected, declines of TSS and so

563 dry matter (DM) were observed during the diafiltration because the membrane did not retain solutes
564 such as sugars and organic acids.

565 Particle size distribution and viscosity of the 8 concentrates varied and two groups could be
566 distinguished: C1, C4, C6, C7 had a mean volume diameter D[4,3], between 59 and 98 µm and a limit
567 viscosity of 3 mPa.s, whereas the D[4,3] of the concentrates C2, C3, C5 and C8 was between 178 and
568 246 µm with a limit viscosity of 13.5 mPa.s. The difference between these two groups was mainly
569 explained by the enzymatic treatment which led to a decrease in particle size and viscosity.

570

571 *Carotenoid analysis*

572

573 Nutritional quality was assessed for the 8 concentrates, in two dimensions: carotenoid content and
574 carotenoid bioaccessibility (**Figure 5**). For an MRR equal to about 4, crossflow microfiltration mainly
575 and logically increased carotenoid content 4 fold, even if a larger dispersion of lycopene content was
576 observed between concentrates. This dispersion could be due to processing. Indeed, the application
577 of high temperatures, the exposure to light or oxygen could induce the decrease of total lycopene or
578 its isomerization into isomers such as 5 *cis*, 9 *cis*, 13 *cis* and 15 *cis* (Cooperstone, Francis, & Schwartz,
579 2016; Urbanoviciene, Bobinaite, Bobinas, & Viskelis, 2017). The high sensitivity to lycopene
580 isomerization could explain dispersion (Honest, Zhang, & Zhang, 2011; Petry & Mercadante, 2017)
581 where all *cis*-isomers appearing from processing contributed to the variation observed in lycopene
582 quantification. Indeed, the percentage of *cis*-isomers from lycopene varied from 1.7% (C8
583 concentrate) to 9.9% (C1 concentrate) for the eight concentrates. The lowest value was obtained for
584 C8 that was the concentrate treated with the mildest conditions (no enzyme treatment, low
585 temperature, low crossflow velocity and no pasteurization). Furthermore, the process induced
586 carotenoid bioaccessibility changes in the concentrates depending on the combination of operating
587 parameters. Indeed, bioaccessibility varied from 15 to 27% for BC, from 20 to 30% for BCX and from
588 0.6 to 1.5% for LYC. These changes were greater for β-cryptoxanthin and β-carotene bioaccessibility

than lycopene bioaccessibility. We can notice that the very low lycopene bioaccessibility for all concentrates did not allow to quantify bioaccessible cis-isomers. So, for lycopene, the cis-isomerization did not affect the bioaccessibility. In fact, the C5 concentrate differed from the others by having the highest BCX and BC bioaccessibility. However, the conditions for obtaining the best carotenoid bioaccessibility were not the same as those that gave the best filtration performance (high and stable J_p). So a compromise will have to be found between carotenoid bioaccessibility and filtration performance.

Vitamin A activity

RAE and RAE* were calculated to assess vitamin A delivered by juice and the 8 concentrates.

Of course, crossflow microfiltration induced an increase of RAE by 4 because of the carotenoid content which was multiplied by 4 by CMF. A portion of 250 g of concentrate provided from 30 to 36 % of RDA, depending on the concentrate. Taking into account the bioaccessibility, RAE* values of concentrates were divided by up to 4.5, as for juices, and provided from 6 to 10 % of RDA. For concentrates, it should be noted that the dispersion of the RAE* was greater than the RAE, which may be explained by a more variable process effect on bioaccessibility than on the carotenoid content alone between concentrates. In fact, although taking into account the fact that bioaccessibility decreased vitamin A intake, microfiltration compensated this decrease and even increased it. Indeed, 250 g of juice provided 1.8 % RDA, whereas after microfiltration, 250 g of concentrate provided up to 10% of RDA (for C5 concentrate). Note that the RAE* was probably underestimated because it was calculated from RAE which was theoretically defined by IOM and already takes into account the bioefficacy of carotenoids (West, Eilander, & van Lieshout, 2002).

3.2.2. Effects of the operating conditions on permeate flux and concentrate quality

Permeate flux and stability

The three most influential parameters on permeate flux have positive effects on it. The importance of their effects was in descending order enzyme dose (84%), filtration temperature T_{CMF} (50%) and crossflow velocity U (45%). These 3 parameters alone explained almost 90% of the cumulated effect of all operating parameters thanks to a decrease in viscosity and membrane fouling. The other parameters, liquefaction temperature and mode (T_{liq} and M_{liq}), as well as diafiltration, did not have a significant effect on permeate flux (2.6%, 2.1% and 1.6% respectively). This last observation is not in accordance with literature where usually the diafiltration step increases J_p slightly. Indeed, feeding with water instead of juice decreases the viscosity and contributes to enhancing permeate flux according to Darcy's law (Basso, Gonçalves, Grimaldi, & Viotto, 2009; Polidori et al., 2018). In this work, diafiltration had no effect on permeate flux probably because the diavolume ratio of 1.0 was too low and the diafiltration was carried out at the end of the microfiltration, when the MRR of 4.4 was already attained.

The three most influential parameters on permeate flux stability were little different from the three most influential parameters on permeate flux. There were in descending order the liquefaction temperature T_{liq} (112.9%), the crossflow velocity U (40.7%) and filtration temperature T_{CMF} (24.0%). Liquefaction temperature accounted for almost 50% of the cumulated effect of all the operating parameters. In addition, contrary to the permeate flux, crossflow velocity (U) and filtration temperature (T_{CMF}) had a negative effect on stability and thus decreased it. Enzymatic treatment had no effect on permeate flux stability (4.6%), whereas it drastically increased permeate flux.

Concentrate characteristics

Pareto charts were used to highlight the relative importance of the seven operating parameter effects on nutritional and structural qualities of concentrates (**Figures 6 and 7**). These charts were made up of two axes: the abscissa axis was the causes (operating parameters) and the ordinate axis was the effect on the response studied (carotenoid bioaccessibility and structural parameters). The

orange curve corresponded to cumulated percentage. Significance threshold could not be determined statistically because of the cumbersome experimental procedure which did not allow to repeat each trials 3 times. Nevertheless, we considered effects below 10% insignificant because of the same order of magnitude as the repeatability.

Enzyme treatment parameters (dose, temperature T_{liq} and mode M_{liq}) were the most influential operating parameters on pro-vitamin A carotenoid bioaccessibility (BC and BCX) (**Figure 6**). T_{liq} and M_{liq} had a positive effect whereas the dose had a negative effect on pro-vitamin A carotenoid bioaccessibility. It was quite different for lycopene bioaccessibility, which was mainly influenced by enzyme dose, filtration temperature (T_{CMF}) and crossflow velocity (U) where dose and T_{CMF} had a negative effect whereas crossflow velocity had a positive effect (**Figure 6**). The operating conditions related to the microfiltration, T_{CMF} and U, had a greater impact on the lycopene bioaccessibility than pro-vitamin A carotenoids. This could be due to the greater sensitivity of lycopene to isomerization and oxidation during food processing (Cooperstone et al., 2016; Urbanoviciene et al., 2017). Note that contrary to our results, recent studies on tomato showed that thermal processing can improve the lycopene bioaccessibility (Colle, Lemmens, Van Buggenhout, Van Loey, & Hendrickx, 2010; Knockaert, Pulissery, et al., 2012). The high shear rate caused by high crossflow velocity during crossflow microfiltration contributed to cell breakdown and therefore to the more effective release of crystalloid lycopene from chromoplasts and lycopene bioaccessibility (R. M. Schweiggert et al., 2012).

Enzyme dose remained the common cause of decreasing in carotenoid bioaccessibility. The enzymatic treatment led to the modification of pectin concentration and structural properties which could promote its interaction with bile salts. Indeed, Cervantes-Paz et al. (2017) explained the possible interaction of low pectin concentration with bile salts can modulate carotenoid bioaccessibility knowing that bile salts are key components of lipid digestion and micelle formation (Cervantes-Paz et al., 2016). For the three carotenoids, pasteurization did not affect carotenoid bioaccessibility which is in accordance with Sentandreu et al. (2020). Even if it appeared significant

for β-carotene, the effect of diafiltration on carotenoid bioaccessibility stayed quiet low. The ability of carotenoids to be incorporated into the micelles depended little or not at all on the major solute fraction. So the step of diafiltration could be interesting to reduce sugar content and therefore to produce healthier concentrates.

Enzyme dose was the largest cause of decrease of D[4,3] and viscosity which account for 60% and 80% respectively of all operating parameters (**Figure 7**). The diafiltration step also contributed to decreasing particle size and viscosity with an effect of over 20%. None of the other parameters had any effect on the structural characteristics studied.

Finally, enzyme dose was clearly the most influential parameter on assessed values resulting in a decrease of carotenoid bioaccessibility, particle size and viscosity and in an increase of permeate flux. On the other hand, no correlation between particle size (D[4,3]), viscosity (η) and bioaccessibility was highlighted, confirming results mentioned by Gence. L et al. (Laura Gence, Servent, Poucheret, Hiol, & Dhuique-Mayer, 2016). These observations were contradictory to literature on citrus juices which indicates that the particle size are strongly linked to carotenoid bioaccessibility (Carla M. Stinco et al., 2012). However, concentrates with high J_p were characterized by low viscosity and low particle size. So, a compromise of enzyme dose would be found to ensure the best carotenoid bioaccessibility while maintaining an acceptable performance for the process. Moreover, the other parameters would be selected in order to give the best carotenoid bioaccessibility (enzyme liquefaction in batch mode at 50°C, T_{CMF} = 30°C, U = 5 $m.s^{-1}$, with diafiltration and no pasteurization).

3.3. Focus on the most influential factor

The last phase aimed to complete the study of the impact of enzyme dose in order to investigate if it is possible to ensure good carotenoid bioaccessibility while maintaining acceptable process performance. For that, a concentrate was produced at MMR 4.4 fixing the best combination of

691 operating conditions for carotenoid bioaccessibility (based on the results obtained from the Plackett-
692 Burman experimental design in the previous phase) and decreasing Ultrazym dose to 50 µL.kg^{-1}. So
693 two trials were carried out with the third lot of juice (lot C) using the production of a concentrate
694 without enzymes as a reference (**Table 6**).

695 A pre-liquefaction with a dose of 50 µL.kg^{-1} of Ultrazym doubled permeate flux. Thanks to this
696 enzyme treatment, J_p remained above 80 g.h^{-1}.m^{-2} up to a MRR of 4.4. This low dose of enzyme was
697 sufficient to ensure high process performance. Furthermore, the permeate flux was very stable for
698 the enzyme treated concentrate compared to the untreated one.

699 The differences of TSS, SIS and DM between the two concentrates were significant ($p < 0.05$) but very
700 slight. The enzymatic treatment with 50 µL.kg^{-1} had the same effect on the viscosity as with 300
701 µL.kg^{-1}: the viscosity was divided by 3 until it reached a value below 3 mPa.s. Regarding particle size,
702 50 µL.kg^{-1} of Ultrazym modified neither the D[4,3] nor the size dispersion (Span) in the concentrate
703 contrary to the treatment with 300 µL.kg^{-1}.

704 In this case, carotenoid bioaccessibility was not affected by enzymatic treatment which differs from
705 previous results that showed enzymatic treatment with 300 µL.kg^{-1} of Ultrazym was the main cause
706 of the decrease in bioaccessibility of β-carotene, β-cryptoxanthin and lycopene. With 50 µL.kg^{-1} of
707 Ultrazym, carotenoid bioaccessibility was preserved and therefore, the RAE* also.

708 The bioaccessibility ratio between initial juices and concentrates, calculated from the 2 main
709 bioaccessible carotenoids (BC and BCX), could be used to compare the last concentrate (with enzyme
710 Table 6) with the C5 concentrate which gave the best bioaccessibilities in the previous part (Table 5).
711 By calculating this ratio, we showed the average bioaccessibility was increased by about 30% in both
712 cases. So the effect of the process on the bioaccessibility of the 2 main carotenoids could be
713 considered as similar.

714 Finally, the final concentrate treated with 50 µL.kg^{-1} of enzymes gave high permeate flux with good
715 carotenoid bioaccessibility. So this enzymatic treatment resulted in an interesting compromise

between process performance and nutritional quality. Further investigations should be considered to refine the optimization of the enzyme dose and also to provide insights for a better understanding of the phenomena involved.

4. Conclusion

In this study, a new process based on crossflow microfiltration was investigated by selecting the operating conditions giving the best nutritional quality of the final concentrate evaluated through its carotenoid potential while guaranteeing a high process performance. Among all the operating conditions, the enzyme dose appeared to play a major role on both permeate flux and carotenoid bioaccessibility in the studied process. Several perspectives could be considered to try to better understand these results such as examining in more detail the impact of pectin structure on carotenoid micellarization or what happens at the cellular level after enzymatic treatment. Other enzymes could also be investigated to compare their effects on cellular structure and to explain the variation of carotenoid bioaccessibility.

Results showed that bioaccessible carotenoid content could be multiplied by 4.5 to 4.8 in the concentrate in comparison with Citrus juice using CMF up to MRR 4.4. Crossflow microfiltration could be easily carried out up to a higher MRR in that case (high permeate flux and no drastic drop vs. MRR) and so the bioaccessible carotenoid content should be easily increased leading to higher nutritional potential of concentrate. In addition, the coupling of microfiltration with other mechanical processes that could favor cell destructuring/destroying and thus carotenoid release from chromoplasts such as homogenization, would be another avenue of research.

Acknowledgements

740 This work was carried out with the financial support of the Centre for International Cooperation in
741 Agronomic Research for development (CIRAD) and the Doctoral School GAIA (Montpellier, France).

742

743 **Declaration of interests**

744 The authors of this work declare no conflict of interest.

745

746

747 **References**

748 Aschoff, J., Rolke, C., Breusing, N., Bosy-Westphal, A., Högel, J., Carle, R., & Schweiggert, R. (2015).
749 Bioavailability of β-cryptoxanthin is greater from pasteurized orange juice than from fresh
750 oranges – a randomized cross-over study. *Molecular nutrition & food research, 59*.
751 doi:10.1002/mnfr.201500327
752 Aschoff, J. K., Kaufmann, S., Kalkan, O., Neidhart, S., Carle, R., & Schweiggert, R. M. (2015). In Vitro
753 Bioaccessibility of Carotenoids, Flavonoids, and Vitamin C from Differently Processed
754 Oranges and Orange Juices [Citrus sinensis (L.) Osbeck]. *Journal of Agricultural and Food*
755 *Chemistry, 63*(2), 578-587. doi:10.1021/jf505297t
756 Barba, F. J., Saraiva, J. M. A., Cravotto, G., & Lorenzo, J. M. (2019). *Innovative Thermal and Non-*
757 *Thermal Processing, Bioaccessibility and Bioavailability of Nutrients and Bioactive*
758 *Compounds*: Woodhead Publishing.
759 Basso, R. C., Gonçalves, L. A. G., Grimaldi, R., & Viotto, L. A. (2009). Degumming and production of
760 soy lecithin, and the cleaning of a ceramic membrane used in the ultrafiltration and
761 diafiltration of crude soybean oil. *Journal of Membrane Science, 330*(1), 127-134.
762 doi:https://doi.org/10.1016/j.memsci.2008.12.052
763 Bungau, S., Abdel-Daim, M. M., Tit, D. M., Ghanem, E., Sato, S., Maruyama-Inoue, M., . . .
764 Kadonosono, K. (2019). Health benefits of polyphenols and carotenoids in age-related eye
765 diseases. *Oxidative medicine and cellular longevity, 2019*.
766 Cervantes-Paz, B., de Jesús Ornelas-Paz, J., Pérez-Martínez, J. D., Reyes-Hernández, J., Zamudio-
767 Flores, P. B., Rios-Velasco, C., . . . Ruiz-Cruz, S. (2016). Effect of pectin concentration and
768 properties on digestive events involved on micellarization of free and esterified carotenoids.
769 *Food Hydrocolloids, 60*, 580-588.
770 Cervantes-Paz, B., Ornelas-Paz, J. d. J., Ruiz-Cruz, S., Rios-Velasco, C., Ibarra-Junquera, V., Yahia, E. M.,
771 & Gardea-Béjar, A. A. (2017). Effects of pectin on lipid digestion and possible implications for
772 carotenoid bioavailability during pre-absorptive stages: A review. *Food Research*
773 *International, 99*, 917-927. doi:https://doi.org/10.1016/j.foodres.2017.02.012
774 Chaparro, L., Dhuique-Mayer, C., Castillo, S., Vaillant, F., Servent, A., & Dornier, M. (2016).
775 Concentration and purification of lycopene from watermelon juice by integrated
776 microfiltration-based processes. *Innovative Food Science & Emerging Technologies, 37*, 153-
777 160. doi:10.1016/j.ifset.2016.08.001
778 Cheryan, M. (1998). Ultrafiltration and microfiltration handbook, Technomic Pub. *Co., Lancaster, PA*.
779 Cilla, A., Alegría, A., de Ancos, B. a., Sánchez-Moreno, C. n., Cano, M. P., Plaza, L., . . . Barberá, R.
780 (2012). Bioaccessibility of tocopherols, carotenoids, and ascorbic acid from milk-and soy-
781 based fruit beverages: influence of food matrix and processing. *Journal of Agricultural and*
782 *Food Chemistry, 60*(29), 7282-7290.
783 Cisse, M., Vaillant, F., Soro, D., Reynes, M., & Dornier, M. (2011). Crossflow microfiltration for the
784 cold stabilization of roselle (Hibiscus sabdariffa L.) extract. *Journal of Food Engineering,*
785 *106*(1), 20-27.
786 Colle, I., Lemmens, L., Van Buggenhout, S., Van Loey, A., & Hendrickx, M. (2010). Effect of thermal
787 processing on the degradation, isomerization, and bioaccessibility of lycopene in tomato
788 pulp. *Journal of Food Science, 75*(9), C753-C759.
789 Cooperstone, J. L., Francis, D. M., & Schwartz, S. J. (2016). Thermal processing differentially affects
790 lycopene and other carotenoids in cis-lycopene containing, tangerine tomatoes. *Food*
791 *Chemistry, 210*, 466-472. doi:https://doi.org/10.1016/j.foodchem.2016.04.078
792 Corredig, M., Kerr, W., & Wicker, L. (2001). Particle size distribution of orange juice cloud after
793 addition of sensitized pectin. *Journal of Agricultural and Food Chemistry, 49*(5), 2523-2526.
794 Dahdouh, L., Delalonde, M., Ricci, J., Rouquie, C., & Wisniewski, C. (2016). *Effect of high shear rates*
795 *on physico-chemical characteristics, rheological behavior and fouling propensity of orange*
796 *juices during cross-flow microfiltration*.
797 Dahdouh, L., Delalonde, M., Ricci, J., Ruiz, E., & Wisnewski, C. (2018). Influence of high shear rate on
798 particles size, rheological behavior and fouling propensity of fruit juices during crossflow

799 microfiltration: Case of orange juice. *Innovative Food Science & Emerging Technologies, 48*,
800 304-312. doi:https://doi.org/10.1016/j.ifset.2018.07.006
801 Dahdouh, L., Wisniewski, C., Ricci, J., Kapitan-Gnimdu, A., Dornier, M., & Delalonde, M. (2015).
802 Development of an original lab-scale filtration strategy for the prediction of microfiltration
803 performance: Application to orange juice clarification. *Separation and Purification*
804 *Technology, 156*, 42-50. doi:https://doi.org/10.1016/j.seppur.2015.10.010
805 de Abreu, F. P., Dornier, M., Dionisio, A. P., Carail, M., Caris-Veyrat, C., & Dhuique-Mayer, C. (2013).
806 Cashew apple (Anacardium occidentale L.) extract from by-product of juice processing: a
807 focus on carotenoids. *Food Chem, 138*(1), 25-31. doi:10.1016/j.foodchem.2012.10.028
808 Dhuique-Mayer, C., Borel, P., Reboul, E., Caporiccio, B., Besancon, P., & Amiot, M. J. (2007). β-
809 Cryptoxanthin from Citrus juices: Assessment of bioaccessibility using an in vitro
810 digestion/Caco-2 cell culture model. *The British journal of nutrition, 97*, 883-890.
811 doi:10.1017/S0007114507670822
812 Dornier, M., Belleville, M.-P., & Vaillant, F. (2018). Membrane Technologies for Fruit Juice Processing.
813 In A. Rosenthal, R. Deliza, J. Welti-Chanes, & G. V. Barbosa-Cánovas (Eds.), *Fruit Preservation:*
814 *Novel and Conventional Technologies* (pp. 211-248). New York, NY: Springer New York.
815 Etcheverry, P., Grusak, M. A., & Fleige, L. E. (2012). Application of in vitro bioaccessibility and
816 bioavailability methods for calcium, carotenoids, folate, iron, magnesium, polyphenols, zinc,
817 and vitamins B6, B12, D, and E. *Frontiers in physiology, 3*, 317.
818 Gates, K. W. (2012). Essentials of Thermal Processing by Gary S. Tucker and Susan Featherstone.
819 *Journal of Aquatic Food Product Technology, 21*(4), 393-400.
820 doi:10.1080/10498850.2012.692660
821 Gence, L., Servent, A., Poucheret, P., Hiol, A., & Dhuique-Mayer, C. (2016). *Citrus juices vs*
822 *concentrates obtained by innovative membrane technology: Bioaccessibility of pro-vitamin A*
823 *carotenoids*.
824 Gence, L., Servent, A., Poucheret, P., Hiol, A., & Dhuique-Mayer, C. (2018). Pectin structure and
825 particle size modify carotenoid bioaccessibility and uptake by Caco-2 cells in citrus juices vs.
826 concentrates. *Food Funct, 9*(6), 3523-3531. doi:10.1039/c8fo00111a
827 Gies, M., Descalzo, A. M., Servent, A., & Dhuique-Mayer, C. (2019). Incorporation and stability of
828 carotenoids in a functional fermented maize yogurt-like product containing phytosterols.
829 *Lwt, 111*, 105-110.
830 Gleize, B., Steib, M., André, M., & Reboul, E. (2012). Simple and fast HPLC method for simultaneous
831 determination of retinol, tocopherols, coenzyme Q10 and carotenoids in complex samples.
832 *Food Chemistry, 134*(4), 2560-2564. doi:https://doi.org/10.1016/j.foodchem.2012.04.043
833 Goupy, J. (2006). *Plans d'expériences*: Ed. Techniques Ingénieur.
834 Hofs, B., Ogier, J., Vries, D., Beerendonk, E. F., & Cornelissen, E. R. (2011). Comparison of ceramic and
835 polymeric membrane permeability and fouling using surface water. *Separation and*
836 *Purification Technology, 79*(3), 365-374.
837 Honest, K. N., Zhang, H. W., & Zhang, L. (2011). Lycopene: Isomerization Effects on Bioavailability and
838 Bioactivity Properties. *Food Reviews International, 27*(3), 248-258.
839 doi:10.1080/87559129.2011.563392
840 Jayani, R. S., Saxena, S., & Gupta, R. (2005). Microbial pectinolytic enzymes: a review. *Process*
841 *Biochemistry, 40*(9), 2931-2944.
842 Knockaert, G., Lemmens, L., Van Buggenhout, S., Hendrickx, M., & Van Loey, A. (2012). Changes in β-
843 carotene bioaccessibility and concentration during processing of carrot puree. *Food*
844 *Chemistry, 133*(1), 60-67. doi:https://doi.org/10.1016/j.foodchem.2011.12.066
845 Knockaert, G., Pulissery, S. K., Colle, I., Van Buggenhout, S., Hendrickx, M., & Van Loey, A. (2012).
846 Lycopene degradation, isomerization and in vitro bioaccessibility in high pressure
847 homogenized tomato puree containing oil: Effect of additional thermal and high pressure
848 processing. *Food Chemistry, 135*(3), 1290-1297.

Kopec, R. E., & Failla, M. L. (2018). Recent advances in the bioaccessibility and bioavailability of carotenoids and effects of other dietary lipophiles. *Journal of Food Composition and Analysis, 68*, 16-30. doi:https://doi.org/10.1016/j.jfca.2017.06.008

Kuddus, M. (2018). *Enzymes in food biotechnology: production, applications, and future prospects*: Academic Press.

Lee, Y., Hu, S., Park, Y.-K., & Lee, J.-Y. (2019). Health Benefits of Carotenoids: A Role of Carotenoids in the Prevention of Non-Alcoholic Fatty Liver Disease. *Preventive nutrition and food science, 24*(2), 103.

Lemmens, L., Van Buggenhout, S., Oey, I., Van Loey, A., & Hendrickx, M. (2009). Towards a better understanding of the relationship between the β-carotene in vitro bio-accessibility and pectin structural changes: a case study on carrots. *Food Research International, 42*(9), 1323-1330.

Macedo, M., Robrigues, R. D. P., Pinto, G. A. S., & de Brito, E. S. (2015). Influence of pectinolyttic and cellulotyc enzyme complexes on cashew bagasse maceration in order to obtain carotenoids. *Journal of Food Science and Technology, 52*(6), 3689-3693. doi:10.1007/s13197-014-1411-x

Maktouf, S., Neifar, M., Drira, S. J., Baklouti, S., Fendri, M., & Châabouni, S. E. (2014). Lemon juice clarification using fungal pectinolytic enzymes coupled to membrane ultrafiltration. *Food and Bioproducts Processing, 92*(1), 14-19.

Medicine, I. o. (2001). *Dietary Reference Intakes for Vitamin A, Vitamin K, Arsenic, Boron, Chromium, Copper, Iodine, Iron, Manganese, Molybdenum, Nickel, Silicon, Vanadium, and Zinc*. Washington, DC: The National Academies Press.

Mierczynska-Vasilev, A., & Smith, P. (2015). Current state of knowledge and challenges in wine clarification. *Australian journal of grape and wine research, 21*, 615-626.

Petry, F. C., & Mercadante, A. Z. (2017). Impact of in vitro digestion phases on the stability and bioaccessibility of carotenoids and their esters in mandarin pulps. *Food & Function, 8*(11), 3951-3963. doi:10.1039/C7FO01075C

Polidori, J., Dhuique-Mayer, C., & Dornier, M. (2018). Crossflow microfiltration coupled with diafiltration to concentrate and purify carotenoids and flavonoids from citrus juices. *Innovative Food Science & Emerging Technologies, 45*, 320-329. doi:https://doi.org/10.1016/j.ifset.2017.11.015

Poulaert, M., Borel, P., Caporiccio, B., Gunata, Z., & Dhuique-Mayer, C. (2012). Grapefruit Juices Impair the Bioaccessibility of β-Carotene from Orange-Fleshed Sweet Potato but Not Its Intestinal Uptake by Caco-2 Cells. *Journal of Agricultural and Food Chemistry, 60*(2), 685-691. doi:10.1021/jf204004c

Rodriguez-Concepcion, M., Avalos, J., Bonet, M. L., Boronat, A., Gomez-Gomez, L., Hornero-Mendez, D., . . . Zhu, C. (2018). A global perspective on carotenoids: Metabolism, biotechnology, and benefits for nutrition and health. *Progress in Lipid Research, 70*, 62-93. doi:https://doi.org/10.1016/j.plipres.2018.04.004

Schweiggert, R., & Carle, R. (2017). Carotenoid deposition in plant and animal foods and its impact on bioavailability. *Critical Reviews in Food Science and Nutrition, 57*(9), 1807-1830.

Schweiggert, R. M., Mezger, D., Schimpf, F., Steingass, C. B., & Carle, R. (2012). Influence of chromoplast morphology on carotenoid bioaccessibility of carrot, mango, papaya, and tomato. *Food Chemistry, 135*(4), 2736-2742.

Sentandreu, E., Stinco, C. M., Vicario, I. M., Mapelli-Brahm, P., Navarro, J. L., & Meléndez-Martínez, A. J. (2020). High-pressure homogenization as compared to pasteurization as a sustainable approach to obtain mandarin juices with improved bioaccessibility of carotenoids and flavonoids. *Journal of Cleaner Production, 262*, 121325. doi:https://doi.org/10.1016/j.jclepro.2020.121325

Servent, A., Abreu, F. A. P., Dhuique-Mayer, C., Belleville, M. P., & Dornier, M. (2020). Concentration and purification by crossflow microfiltration with diafiltration of carotenoids from a by-product of cashew apple juice processing. Innovative Food Science and Emerging Technologies, 66, 102519.

Stinco, C. M., Fernández-Vázquez, R., Escudero-Gilete, M. L., Heredia, F. J., Meléndez-Martínez, A. J., & Vicario, I. M. (2012). Effect of Orange Juice's Processing on the Color, Particle Size, and Bioaccessibility of Carotenoids. *Journal of Agricultural and Food Chemistry, 60*(6), 1447-1455. doi:10.1021/jf2043949

Stinco, C. M., Pumilia, G., Giuffrida, D., Dugo, G., Meléndez-Martínez, A. J., & Vicario, I. M. (2019). Bioaccessibility of carotenoids, vitamin A and α-tocopherol, from commercial milk-fruit juice beverages: contribution to the recommended daily intake. *Journal of Food Composition and Analysis, 78*, 24-32.

Sun, Y., Tao, W., Huang, H., Ye, X., & Sun, P. (2019). Flavonoids, phenolic acids, carotenoids and antioxidant activity of fresh eating citrus fruits, using the coupled in vitro digestion and human intestinal HepG2 cells model. *Food Chemistry, 279*, 321-327. doi:https://doi.org/10.1016/j.foodchem.2018.12.019

Tyssandier, V., Lyan, B., & Borel, P. (2001). Main factors governing the transfer of carotenoids from emulsion lipid droplets to micelles. *Biochimica et Biophysica Acta (BBA) - Molecular and Cell Biology of Lipids, 1533*(3), 285-292. doi:https://doi.org/10.1016/S1388-1981(01)00163-9

Urbanoviciene, D., Bobinaite, R., Bobinas, C., & Viskelis, P. (2017). *Stability and isomerisation of lycopene in oil-based model system during accelerated shelf-life testing.* Paper presented at the 11th Baltic Conference on Food Science and Technology" Food science and technology in a changing world" FOODBALT 2017, Jelgava, Latvia, 27-28 April 2017.

Ushikubo, F. Y., Watanabe, A. P., & Viotto, L. A. (2007). Microfiltration of umbu (Spondias tuberosa Arr. Cam.) juice. *Journal of Membrane Science, 288*(1-2), 61-66.

Vaillant, F., Millan, P., O'Brien, G., Dornier, M., Decloux, M., & Reynes, M. (1999). Crossflow microfiltration of passion fruit juice after partial enzymatic liquefaction. *Journal of Food Engineering, 42*(4), 215-224. doi:https://doi.org/10.1016/S0260-8774(99)00124-7

Vaillant, F., Pérez, A. M., Acosta, O., & Dornier, M. (2008). Turbidity of pulpy fruit juice: A key factor for predicting cross-flow microfiltration performance. *Journal of Membrane Science, 325*(1), 404-412.

Vanaja, K., & Shobha Rani, R. (2007). Design of experiments: concept and applications of Plackett Burman design. *Clinical research and regulatory affairs, 24*(1), 1-23.

West, C. E., Eilander, A., & van Lieshout, M. (2002). Consequences of revised estimates of carotenoid bioefficacy for dietary control of vitamin A deficiency in developing countries. *The Journal of nutrition, 132*(9), 2920S-2926S.

Yu, J., & Lencki, R. (2004). Effect of enzyme treatments on the fouling behavior of apple juice during microfiltration. *Journal of Food Engineering, 63*(4), 413-423.

Zhang, Y., Liu, Y., Liu, F., Zheng, X., Xie, Z., Ye, J., . . . Zeng, Y. (2019). Investigation of chromoplast ultrastructure and tissue-specific accumulation of carotenoids in citrus flesh. *Scientia Horticulturae, 256*, 108547. doi:https://doi.org/10.1016/j.scienta.2019.108547

Figure captions

Figure 1. Process flow diagram of the experimental setup (see abbreviation list for meanings).

Figure 2. Effect of crossflow microfiltration (T_{CMF} = 30°C, U = 5 m.s^{-1}, TmP = 2.6 bar, obtained at MRR = 1 with the 4 membranes mounted in series) and enzymatic treatment (300 µL.kg^{-1}, t_{liq} = 90 min, T_{liq} = 30°C, M_{liq} = batch) on the mean volume diameter D[4,3] and span of particles in the products: raw Juice (Lot A), enzyme treated juices with Ultrazym (Juice-Ult) and Pectinex (Juice-Pec), retentates of

945 microfiltration without enzyme (Juice CMF), with enzyme treatments (Juice-Ult CMF and Juice-Pec
946 CMF). Values with the same letters were not significantly different at $p < 0.05$.

947 **Figure 3.** Effect of crossflow microfiltration (T_{CMF} = 30°C, U = 5 $m.s^{-1}$, TmP = 2.6 bar, obtained at MRR
948 = 1 with the 4 membranes mounted in series) and enzymatic treatment (300 $\mu L.kg^{-1}$, t_{liq} = 90 min, T_{liq}
949 = 30°C, M_{liq}= batch) on limit apparent viscosity for a shear rate of 1000 s^{-1} of the products: raw Juice
950 (Lot A), enzyme treated juices with Ultrazym (Juice-Ult) and Pectinex (Juice-Pec), retentates of
951 microfiltration without enzyme (Juice CMF), with enzyme treatments (Juice-Ult CMF and Juice-Pec
952 CMF). Values with the same letters were not significantly different at $p < 0.05$.

953 **Figure 4.** Effect of transmembrane pressure (TmP) on permeate flux (J_p) during crossflow
954 microfiltration of the juice (T_{CMF} = 30°C, U = 5 $m.s^{-1}$, MRR = 1) after enzymatic treatment (Pectinex 300
955 $\mu L.kg^{-1}$, t_{liq} = 90 min, T_{liq} = 30°C, M_{liq} = batch) using the four chosen membranes (Lot A).

956 **Figure 5.** Carotenoid content and bioaccessibility of the eight concentrates (Lot B) obtained according
957 to the combination of different parameters. C# is the concentrate corresponding to the essay #
958 according to the Plackett-Burman design (Mean and standard deviation from 3 repetitions).

959 **Figure 6.** Relative effect of operating parameters on carotenoid bioaccessibility (BC: β-carotene, BCX:
960 β-cryptoxanthin, LYC: lycopene) of concentrates (Lot B). Dose: enzyme dose, Mliq: liquefaction mode,
961 Tliq: liquefaction temperature, TCMF: crossflow microfiltration temperature, U: crossflow velocity,
962 Diaf: diafiltration, Past: pasteurization.

963 **Figure 7.** Relative effects of operating parameters on particle size distribution D[4,3] and viscosity of
964 concentrates (Lot B). Dose: enzyme dose, Mliq: liquefaction mode, Tliq: liquefaction temperature,
965 TCMF: crossflow microfiltration temperature, U: crossflow velocity, Diaf: diafiltration, Past:
966 pasteurization.

967 **Supplementary files**

968 **Table S1.** pH, TA, TSS, SIS, TDM, turbidity in the juice (Lot A), Juice CMF the retentate of
969 microfiltration (T_{CMF} = 30°C, U = 5 $m.s^{-1}$, TmP = 2.6 bar, obtained at MRR = 1 with the 4 membranes
970 mounted in series), Juice-Ult and Juice-Pec the enzyme treated juices with Ultrazym and Pectinex
971 (300 $\mu L.kg^{-1}$, t_{liq} = 90 min, T_{liq} = 30°C, M_{liq} = batch), Juice-Ult and Juice-Pec the enzyme treated juices
972 with Ultrazym and Pectinex microfiltered

973 **Figure S1.** Particle size distribution in the Juice (Lot A), Juice CMF the retentate of microfiltration
974 (T_{CMF} = 30°C, U = 5 $m.s^{-1}$, TmP = 2.6 bar, obtained at MRR = 1 with the 4 membranes mounted in
975 series), Juice-Ult and Juice-Pec the enzyme treated juices with Ultrazym and Pectinex (300 $\mu L.kg^{-1}$, t_{liq}
976 = 90 min, T_{liq} = 30°C, M_{liq} = batch).

977 **Figure S2.** Evolution of permeate flux according the MRR for three concentrates as examples C4, C5
978 and C8.

979

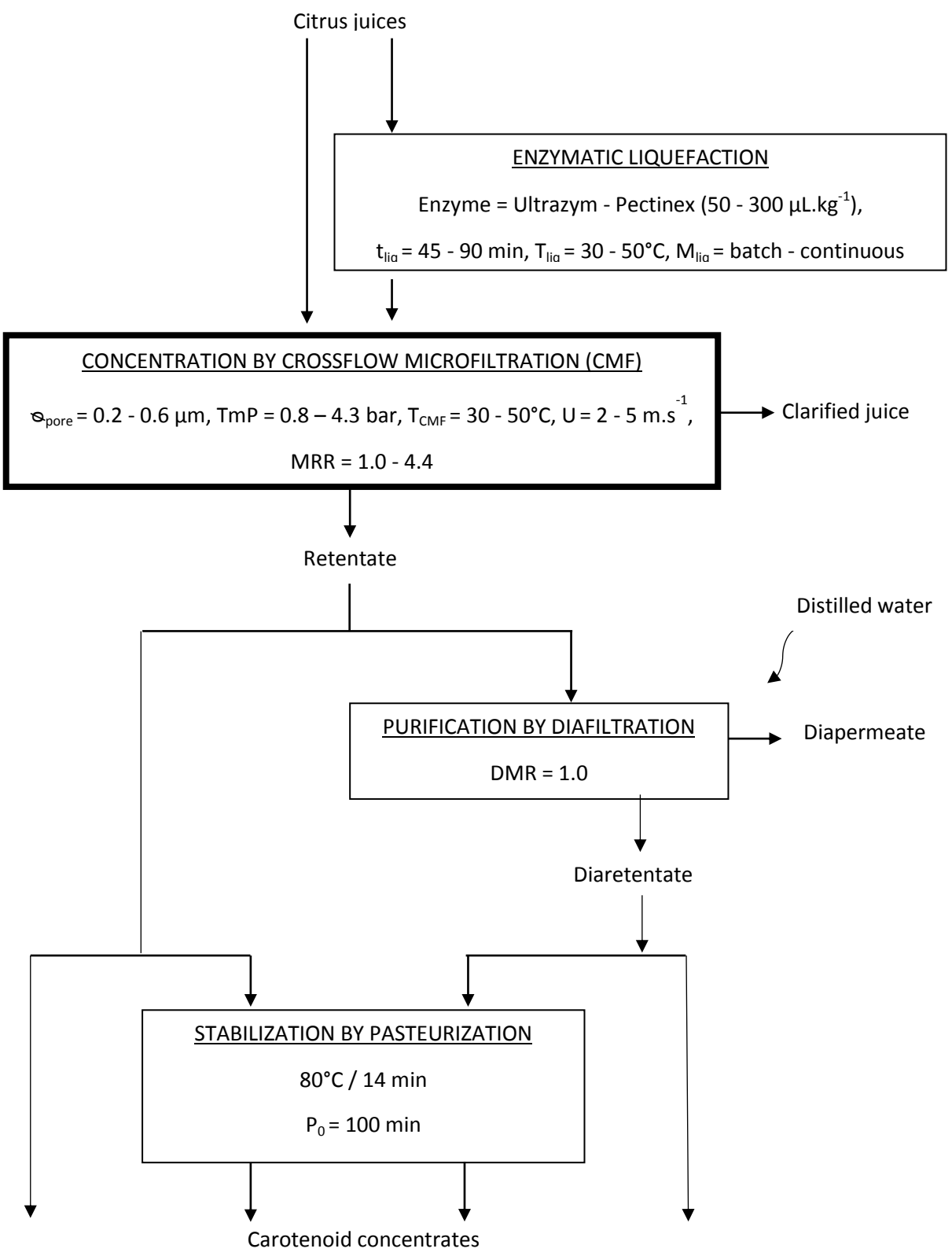

Figure 1. Process flow diagram of the experimental setup (see abbreviation list for meaning).

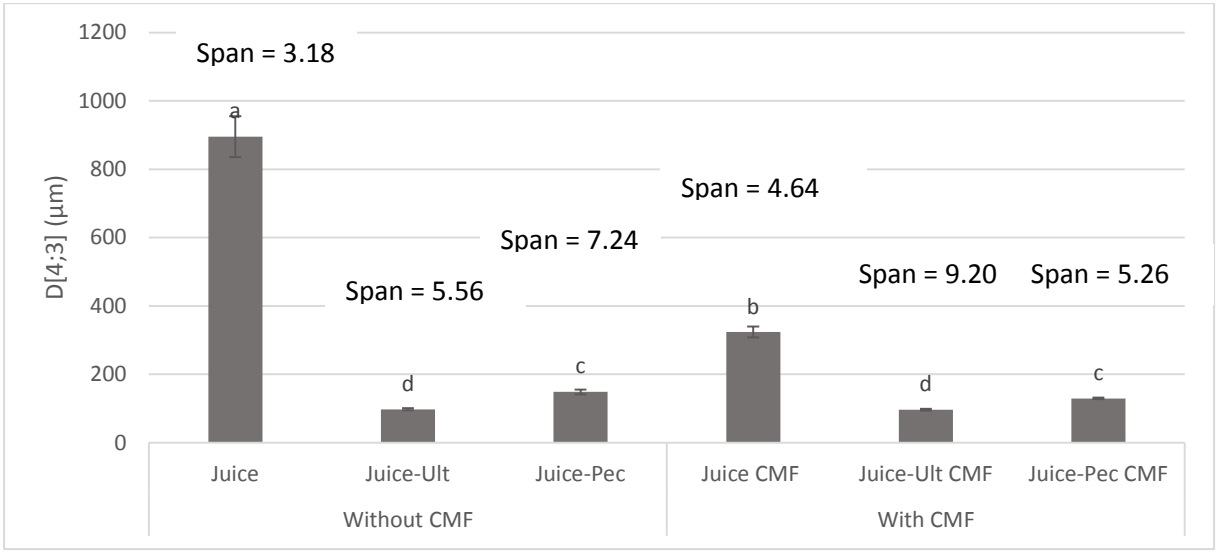

***Figure 2**. Effect of crossflow microfiltration (T_{CMF} = 30°C, U = 5 m.s^{-1}, TmP = 2.6 bar, obtained at MRR = 1 with the 4 membranes mounted in series) and enzymatic treatment (300 µL.kg^{-1}, t_{liq} = 90 min, T_{liq} = 30°C, M_{liq} = batch) on the mean volume diameter D[4,3] and span of particles in the products: raw Juice (Lot A), enzyme treated juices with Ultrazym (Juice-Ult) and Pectinex (Juice-Pec), retentates of microfiltration without enzyme (Juice CMF), with enzyme treatments (Juice-Ult CMF and Juice-Pec CMF). Values with the same letters were not significantly different at p < 0.05.*

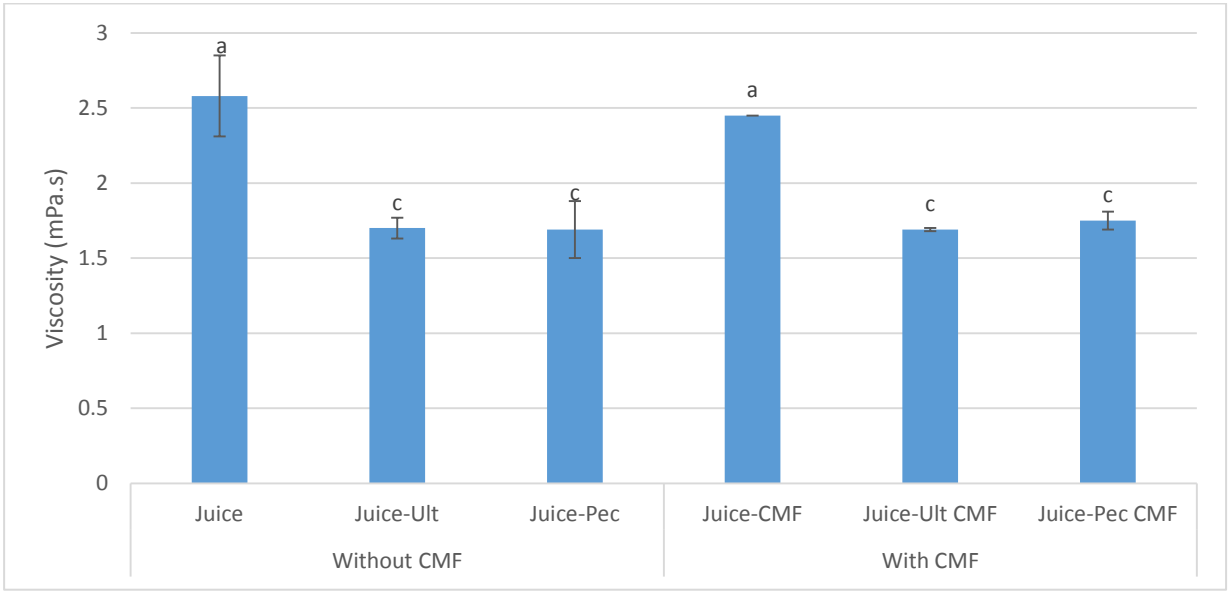

***Figure 3.** Effect of crossflow microfiltration (T_{CMF} = 30°C, U = 5 m.s^{-1}, TmP = 2.6 bar, obtained at MRR = 1 with the 4 membranes mounted in series) and enzymatic treatment (300 µL.kg^{-1}, t_{liq} = 90 min, T_{liq} = 30°C, M_{liq}= batch) on limit apparent viscosity for a shear rate of 1000 s^{-1} of the products: raw Juice (Lot A), enzyme treated juices with Ultrazym (Juice-Ult) and Pectinex (Juice-Pec), retentates of microfiltration without enzyme (Juice CMF), with enzyme treatments (Juice-Ult CMF and Juice-Pec CMF). Values with the same letters were not significantly different at p < 0.05.*

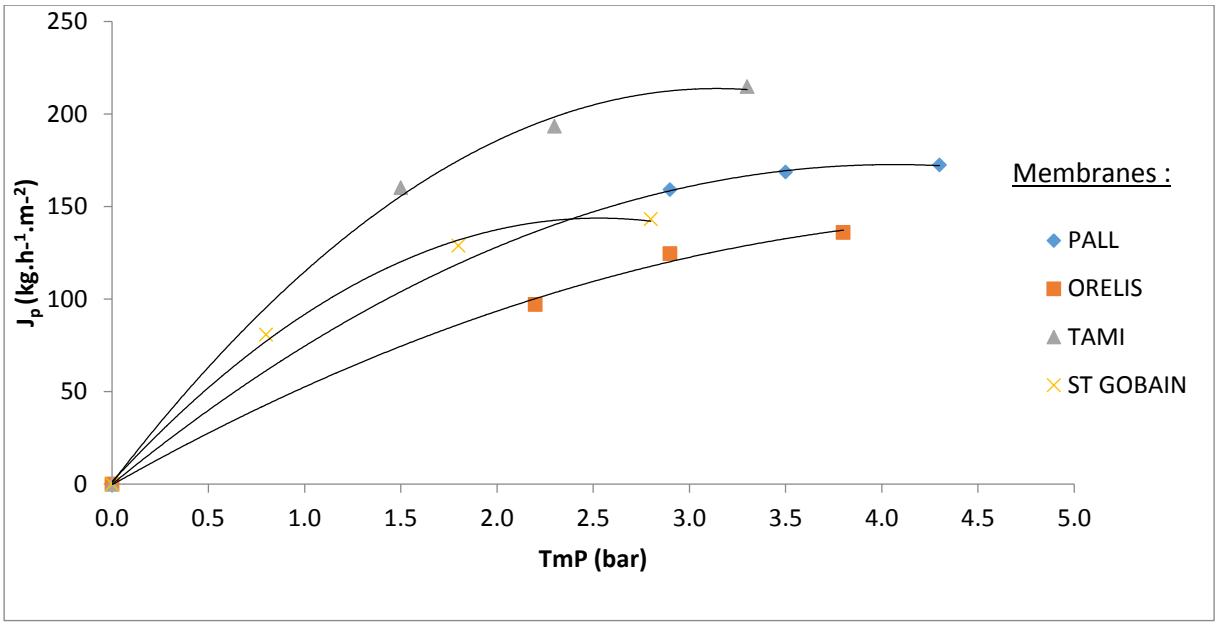

Figure 4. Effect of transmembrane pressure (TmP) on permeate flux (J_p) during crossflow microfiltration of the juice (T_{CMF} = 30°C, U = 5 m.s^{-1}, MRR = 1) after enzymatic treatment (Pectinex 300 µL.kg^{-1}, t_{liq} = 90 min, T_{liq} = 30°C, M_{liq} = batch) using the four chosen membranes (Lot A).

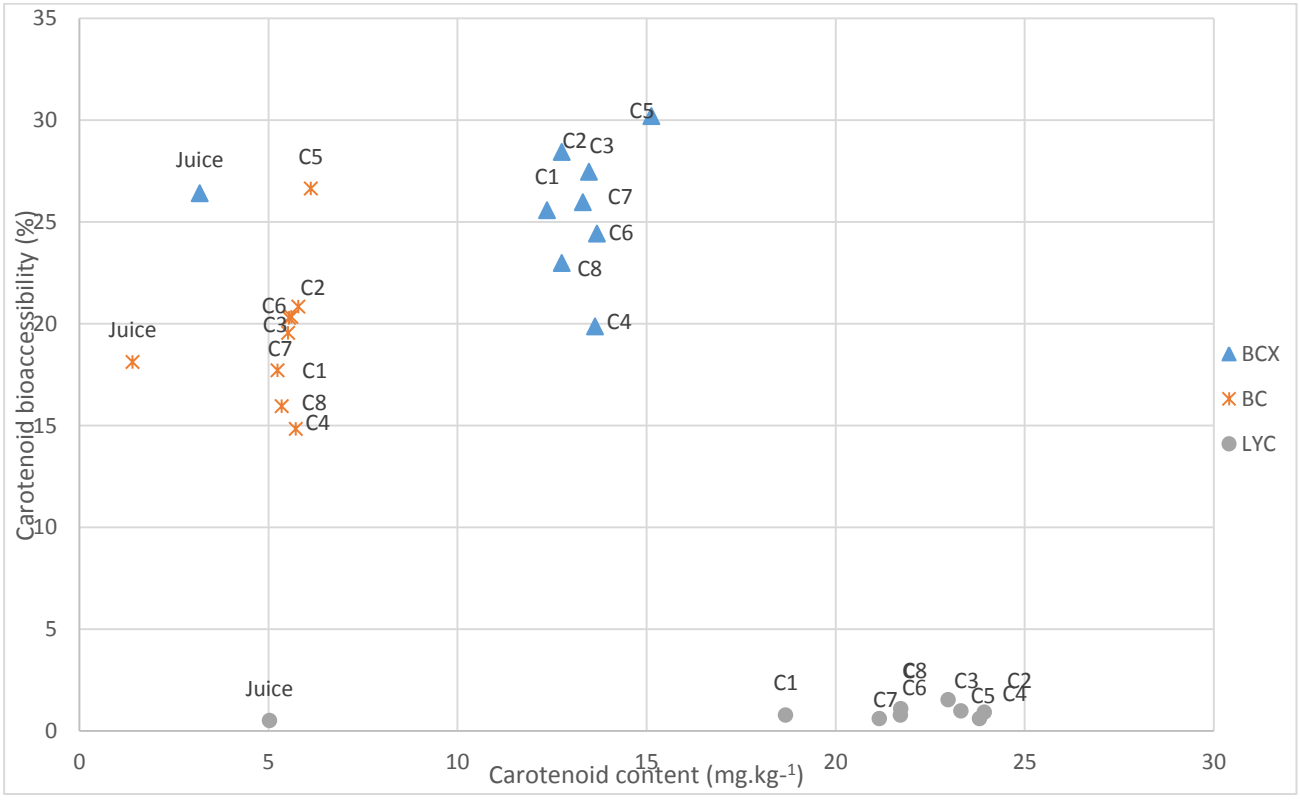

Figure 5. Carotenoid content and bioaccessibility of the eight concentrates (Lot B) obtained according to the combination of different parameters. C# is the concentrate corresponding to the essay # according to the Plackett-Burman design.

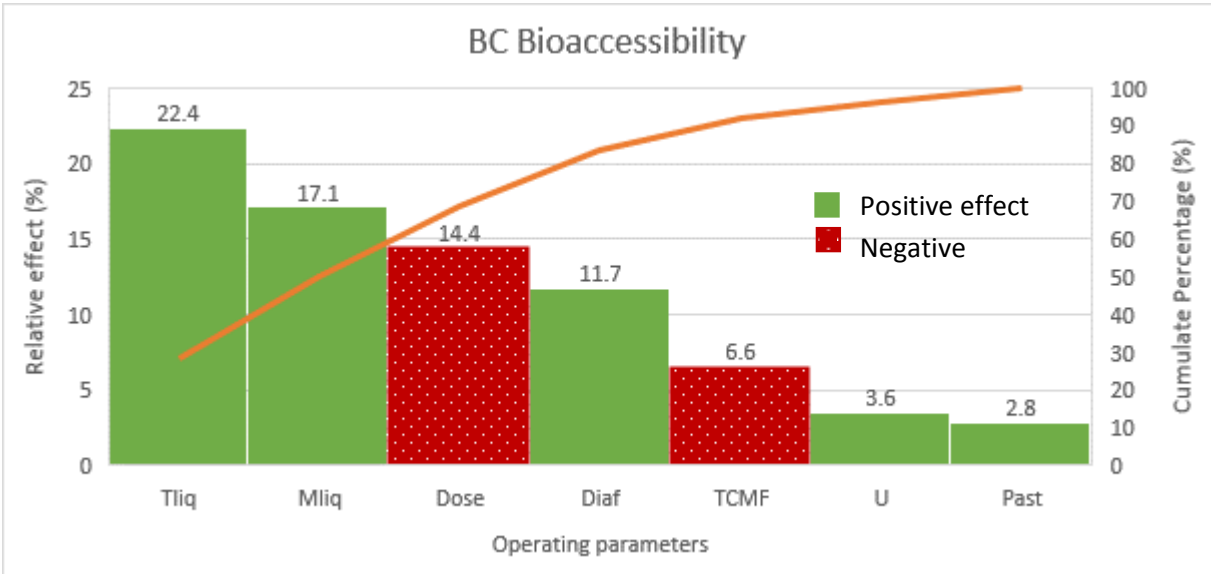

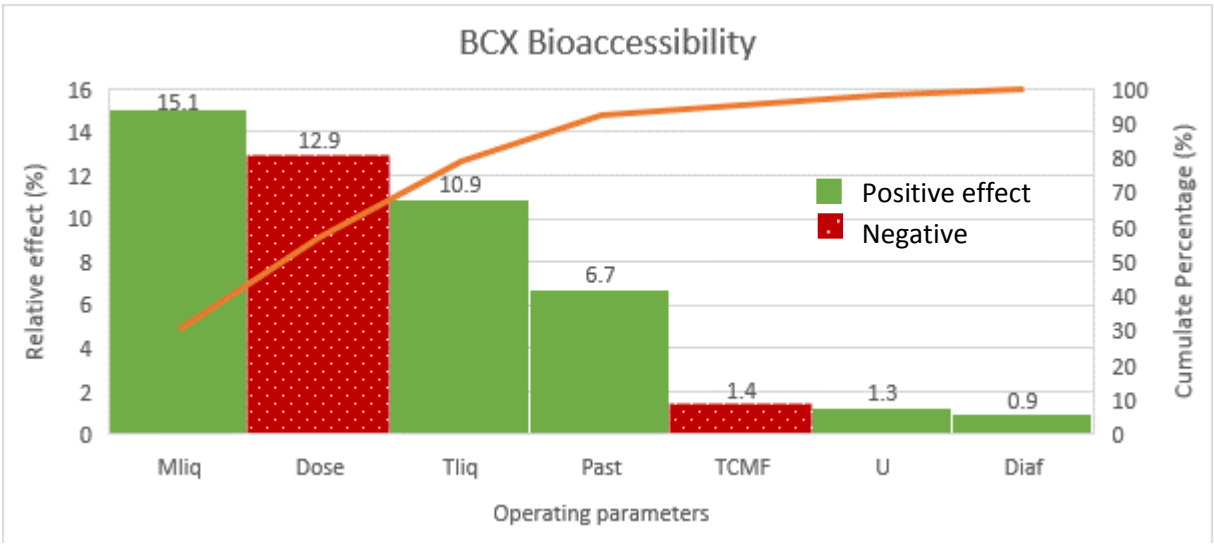

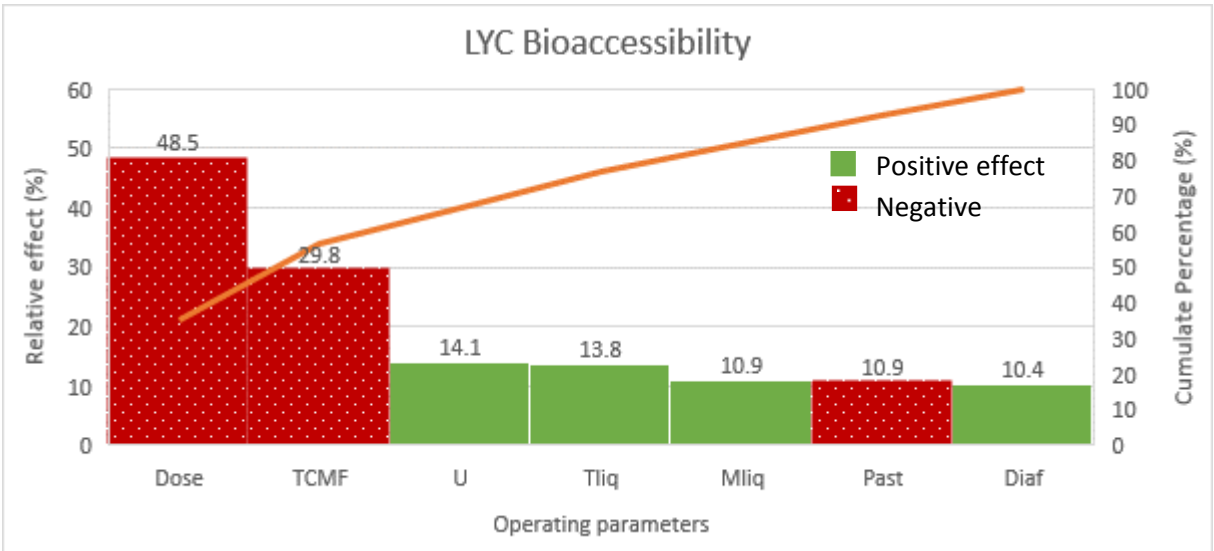

Figure 6. Relative effect of operating parameters on carotenoid bioaccessibility (BC: β-carotene, BCX: β-cryptoxanthin, LYC: lycopene) of concentrates (Lot B). Dose: enzyme dose, Mliq: liquefaction mode, Tliq: liquefaction temperature, TCMF: crossflow microfiltration temperature, U: crossflow velocity, Diaf: diafiltration, Past: pasteurization.

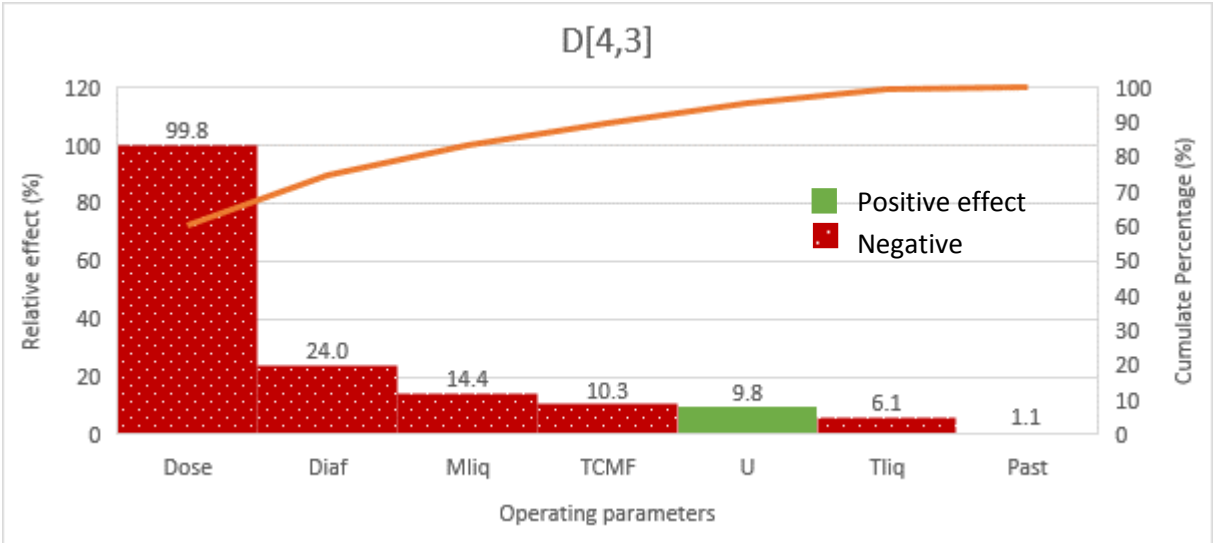

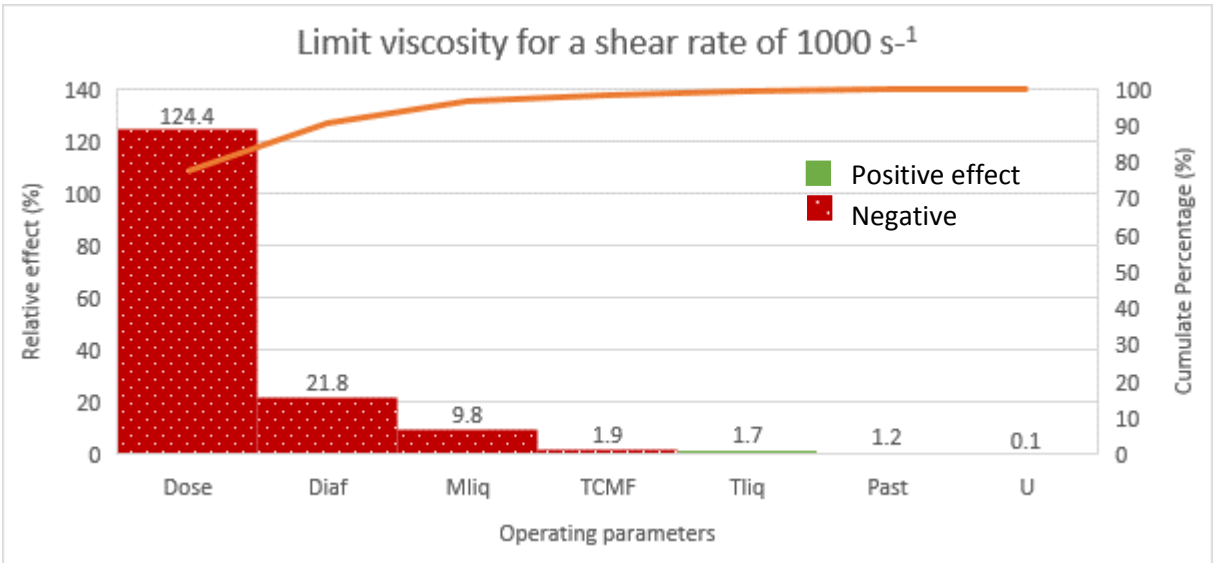

Figure 7. Relative effects of operating parameters on particle size distribution D[4,3] and viscosity of concentrates (Lot B). Dose: enzyme dose, Mliq: liquefaction mode, Tliq: liquefaction temperature, TCMF: crossflow microfiltration temperature, U: crossflow velocity, Diaf: diafiltration, Past: pasteurization.

Table 1. Main characteristics of the 4 tubular membranes chosen for crossflow microfiltration

Manufacturer	Pall-Exekia (Bazet, France)	Orelis (Salindres, France)	Tami Industries (Nyons, France)	Saint-Gobain (Cavaillon, France)
Material of active layer	Alumina (Al_2O_3)	Zirconia (ZiO_2)	Titanium oxide (TiO_2)	Silicon carbide (SiC)
Average pore size (µm)	0.2	0.2	0.2	0.6
Internal diameter (mm)	7	7	7	6
Filtration area (cm^2)	55	55	55	43
Length (m)	0.25	0.25	0.25	0.25
Pristine membrane water permeability ($kg.h^{-1}.m^{-2}.bar^{-1}$)[1]	1500 -1800	≈ 2000	2500 - 3500	≈ 5000
Average stabilized water permeability ($kg.h^{-1}.m^{-2}.bar^{-1}$)[2]	374 (102)	304 (62)	484 (132)	950 (257)

[1] from the suppliers, at 25 °C.

[2] mean and standard deviation measured after at least 6 cleaning cycles, with tap water at 30°C, at TmP ranging from 2.5 bar to 3.4 bar and at U = 5 $m.s^{-1}$. Values used to verify cleaning efficiency after each trial.

Table 2. Plackett-Burman experimental design used to identify the most influent operating parameters (Tami membrane, TmP = 2.6 bar, Ultrazym used as enzyme)

	Concentrates	**C1**	**C2**	**C3**	**C4**	**C5**	**C6**	**C7**	**C8**
Operating parameters	**Enzyme dose** ($\mu L.kg^{-1}$)	300	0	0	300	0	300	300	0
	Liquefaction Mode M_{liq}	Batch	Batch	Continuous	Continuous	Batch	Continuous	Batch	Continuous
	Liquefaction temperature T_{liq} (°C)	30	30	50	30	50	50	50	30
	Filtration temperature T_{CMF} (°C)	30	50	50	50	30	30	50	30
	Crossflow velocity U ($m.s^{-1}$)	5	2	5	5	5	2	2	2
	Diafiltration	No	Yes	No	Yes	Yes	Yes	No	No
	Pasteurization	Yes	Yes	Yes	No	No	Yes	No	No

1063 **Table 3.** Physico-chemical, structural characteristics and carotenoid content and bioaccessibility of
1064 initial citrus juice (mean and standard deviation from n = 3).

		Lot A	Lot B	Lot C
pH		3.51 (0.15)	3.45 (0.02)	3.49 (0.08)
TA ($g.kg^{-1}$)		8.6 (0.2)	10.4 (0.5)	10.8 (0.6)
TSS ($g.kg^{-1}$)		99.8 (1.6)	108.0 (0.1)	111.3 (1.1)
SIS ($g.kg^{-1}$)		3.2 (0.2)	3.1 (0.2)	3.1 (0.3)
TDM ($g.kg^{-1}$)		100.9 (2.0)	110.9 (1.0)	105.0 (0.1)
Limit viscosity (1000 s^{-1}) (mPa.s)		2.43 (0.13)	3.24 (0.24)	2.96 (0.09)
D[4,3] (µm)		896 (60)	912 (17)	922 (21)
Span		3.18 (0.53)	3.12 (0.47)	3.16 (0.27)
Turbidity (NTU)		2169 (147)	3840 (165)	ND
Carotenoid Content ($mg.kg^{-1}$)	BC	ND	1.41 (0.04)	1.17 (0.03)
	BCX	ND	3.19 (0.35)	2.52 (0.02)
	LYC	ND	5.03 (0.16)	6.07 (0.10)
Carotenoid Bioaccessibility β (%)	BC	ND	18.12 (0.51)	12.92 (0.43)
	BCX	ND	26.41 (0.50)	22.70 (0.71)
	LYC	ND	0.51 (0.02)	0.75 (0.13)
RAE (µg/ 250g of juice)		ND	62.6 (4.5)	50.6 (0.8)
RAE* (µg/ 250g of juice)		ND	14.1 (1.4)	9.1 (0.4)
RDA (%)		ND	7.8 (0.6)	6.3 (0.1)

1065 *Not determined.

1066

1067

1068 **Table 4.** Effect of enzymatic treatment (300 µL.kg^{-1}, t_{liq} = 90 min, T_{liq} = 30°C, M_{liq} = batch) on the
1069 stabilized permeate flux J_p during the microfiltration (T_{CMF} = 30°C, MRR = 1) of citrus juice (Lot A) for
1070 different membrane / transmembrane pressure combinations.

J_p (kg.h^{-1}.m^{-2})	PALL (3.5 bar)	ORELIS (2.9 bar)	TAMI (2.3 bar)	SAINT-GOBAIN (1.8 bar)
Raw juice	109.7	105.8	155.2	122.7
Treated with Ultrazym	165.7	113.6	185.8	130.2
Treated with Pectinex	168.7	124.5	193.3	128.8

1071

1072

1073

1074 **Table 5.** Average permeate flux (J_p), physico-chemical and structural characteristics and carotenoid
1075 analysis of the 8 concentrates obtained according to the combination of different parameters (lot B).
1076 C# is the concentrate corresponding to the Plackett-Burman design (Table 2) using the Tami
1077 membrane, TmP = 2.6 bar and Ultrazym as enzyme (Mean and standard deviation from 3).

		C1	C2	C3	C4	C5	C6	C7	C8
J_p (3 < MRR < 4.4) ($kg.h^{-1}.m^{-2}$)		76.1	28.1	55.6	120.8	38.3	48.2	92.1	15.3
Flux instability $\partial Jp/\partial MRR$ (3 < FRM < 4.4) ($kg.h^{-1}.m^{-2}$)		1.6	2.4	9.6	4.5	8.0	7.6	5.6	0.2
TSS ($g.kg^{-1}$)		126.0^{a} (2.6)	51.7^{b} (0.6)	119.3^{c} (0.6)	49.3^{b} (1.2)	51.3^{b} (1.5)	59.7^{d} (0.6)	125.0^{a} (1)	122.0^{e} (2)
SIS ($g.kg^{-1}$)		12.2^{ef} (0.1)	14.7^{a} (0.4)	13.7^{b} (0.5)	12.9^{cd} (0.1)	13.1^{c} (0.2)	12.8^{cd} (0.0)	12.0^{f} (0.5)	12.6^{de} (0.2)
TDM ($g.kg^{-1}$)		115.4^{bc} (0.6)	62.1^{d} (0.4)	117.3^{b} (2.2)	51.4^{f} (1.4)	60.0^{d} (1.7)	53.9^{e} (1.0)	114.9^{c} (1.0)	120.6^{a} (1.0)
Limit viscosity (1000 s^{-1}) (mPa.s)		3.66^{a} (0.03)	11.93^{b} (0.21)	14.67^{c} (0.06)	2.42^{d} (0.05)	12.13^{e} (0.15)	2.81^{d} (0.08)	3.54^{f} (0.03)	14.57^{c} (0.25)
D[4,3] (µm)		98^{a} (4)	178^{b} (6)	238^{c} (21)	68^{d} (2)	196^{e} (10)	62^{d} (1)	59^{d} (4)	246^{c} (26)
Span		6.22 (0.58)	3.91 (0.24)	4.18 (0.59)	8.54 (0.65)	2.24 (0.10)	10.98 (0.28)	5.76 (0.65)	4.48 (0.56)
Turbidity (NTU)		16367^{a} (90)	19110^{b} (385)	15570^{c} (576)	13730^{d} (337)	15850^{ac} (311)	14280^{d} (171)	16020^{ac} (259)	16993^{ae} (200)
Carotenoid Content ($mg.kg^{-1}$)	BC	5.24^{a} (0.13)	5.79^{ab} (0.12)	5.55^{ab} (0.73)	5.73^{ab} (0.51)	6.12^{b} (0.09)	5.61^{ab} (0.21)	5.52^{a} (0.11)	5.35^{b} (0.15)
	BCX	12.37^{c} (0.04)	12.76^{bc} (1.19)	13.48^{bc} (1.21)	13.64^{b} (1.14)	15.13^{a} (0.67)	13.69^{b} (0.40)	13.32^{bc} (0.26)	12.76^{bc} (1.19)
	LYC	18.68^{d} (0.37)	23.94^{a} (1.47)	23.32^{abc} (2.39)	23.81^{ab} (0.74)	22.98^{abc} (0.93)	21.72^{bc} (1.26)	21.16^{c} (0.45)	21.73^{bc} (1.16)
Carotenoid Bioaccessibility β_i (%)	BC	17.71^{cd} (2.10)	20.84^{b} (3.05)	20.28^{bc} (3.62)	14.83^{d} (1.85)	26.64^{a} (1.93)	20.33^{bc} (4.00)	19.55^{bcd} (1.88)	15.95^{cd} (2.46)
	BCX	25.57^{bc} (1.76)	28.43^{b} (1.88)	27.46^{b} (2.36)	19.87^{d} (2.38)	30.20^{a} (0.39)	24.42^{bc} (2.46)	25.96^{b} (2.46)	22.97^{cd} (2.66)
	LYC	0.78^{c} (0.07)	0.91^{b} (0.12)	0.97^{b} (0.14)	0.60^{c} (0.17)	1.53^{a} (0.01)	0.77^{c} (0.14)	0.60^{c} (0.05)	1.09^{b} (0.17)
RAE (µg/ 250g of concentrate)		238.0 (3.1)	253.5 (14.9)	256.0 (27.8)	261.5 (22.5)	285.1 (25.7)	259.5 (8.5)	253.8 (5.0)	244.4 (15.5)
RAE* (µg/ 250g of concentrate)		52.3 (5.2)	62.9 (10.2)	62.0 (14.1)	45.9 (9.5)	81.5 (10.2)	58.6 (10.1)	58.5 (6.7)	48.3 (9.6)
RDA (%)		29.8 (0.4)	31.7 (1.9)	32.0 (3.5)	32.7 (2.8)	35.6 (3.2)	32.4 (1.1)	31.7 (0.6)	30.6 (1.9)
RDA* (%)		6.5 (0.7)	7.9 (1.3)	7.8 (1.8)	5.7 (1.2)	10.2 (1.3)	7.3 (1.3)	7.3 (0.8)	6.0 (1.2)

Table 6. Impact of a low enzyme dose on average permeate flux (J_p) and characteristics of concentrates obtained in the most favorable conditions for carotenoid bioaccessibility (enzyme liquefaction in batch mode at 50°C, T_{CMF} = 30°C, U = 5.m.s^{-1}, with diafiltration and no pasteurization) (Lot C) (Mean and standard deviation from 3 repetitions).

		Concentrate without enzyme (reference)	Concentrate after Ultrazym liquefaction at 50 µL.kg^{-1}
J_p (3 < FRM < 4.4) (kg.h^{-1}.m^{-2})		40.5	81.4
Flux instability $\partial J_p/\partial$MRR (3 < FRM < 4.4) (kg.h^{-1}.m^{-2})		6.2	1.2
TSS (g.kg^{-1})		50.3^{a} (0.6)	53.3^{b} (0.6)
SIS (g.kg^{-1})		10.9^{a} (0.1)	10.7^{a} (0.3)
TDM (g.kg^{-1})		57.5^{a} (0.1)	58.3^{b} (0.1)
Limit viscosity (1000 s^{-1}) (mPa.s)		9.26^{a} (0.08)	2.64^{b} (0.08)
D[4,3] (µm)		233^{a} (17)	230^{a} (11)
Span		3.41 (0.43)	3.51 (0.32)
Carotenoid Content (mg.kg^{-1})	BC	3.87^{a} (0.11)	4.00^{a} (0.21)
	BCX	9.07^{a} (0.13)	8.96^{a} (0.37)
	LYC	20.41^{a} (0.83)	21.78^{a} (1.00)
Carotenoid Bioaccessibility β (%)	BC	15.79 ^{a} (1.47)	16.60^{a} (0.45)
	BCX	27.02^{a} (3.18)	29.43^{a} (2.26)
	LYC	0.94^{a} (0.13)	0.89^{a} (0.05)
RAE (µg/ 250g of concentrate)		175.1 (3.7)	176.7 (8.2)
RAE* (µg/ 250g of concentrate)		38.3 (4.9)	41.3 (4.3)
RDA (%)		21.9	22.1
RDA* (%)		4.8	5.2